CRC Report No. AVFL-27

Heat of Vaporization Measurements of Gasoline and Ethanol Blends Phase 1, Parts A & B

Final Report

August 2016

COORDINATING RESEARCH COUNCIL, INC.
5755 NORTH POINT PARKWAY • SUITE 265 • ALPHARETTA, GA 30022

The Coordinating Research Council, Inc. (CRC) is a non-profit corporation supported by the petroleum and automotive equipment industries. CRC operates through the committees made up of technical experts from industry and government who voluntarily participate. The four main areas of research within CRC are: air pollution (atmospheric and engineering studies); aviation fuels, lubricants, and equipment performance, heavy-duty vehicle fuels, lubricants, and equipment performance (e.g., diesel trucks); and light-duty vehicle fuels, lubricants, and equipment performance (e.g., passenger cars). CRC's function is to provide the mechanism for joint research conducted by the two industries that will help in determining the optimum combination of petroleum products and automotive equipment. CRC's work is limited to research that is mutually beneficial to the two industries involved. The final results of the research conducted by, or under the auspices of, CRC are available to the public.

CRC makes no warranty expressed or implied on the application of information contained in this report. In formulating and approving reports, the appropriate committee of the Coordinating Research Council, Inc. has not investigated or considered patents which may apply to the subject matter. Prospective users of the report are responsible for protecting themselves against liability for infringement of patents.

Foreword

CRC Project No. AVFL-27 was conducted by two contractors, the National Renewable Energy Laboratory in Golden, CO (Part A), and the University of Delaware in Newark, DE (Part B). Both Contractor Final Reports are presented here with an overview Executive Summary prepared by the CRC Advanced Vehicle/Fuel/Lubricants Committee. Part A begins immediately following the AVFL Committee's Executive Summary with the text body and appendices spanning pages 1-28. Part B begins immediately following Part A with the report spanning newly numbered pages 1-31. See the respective Part A and Part B Tables of Contents for details on the placement of the information presented in the two reports.

AVFL Committee Executive Summary

This report documents the efforts and results of two studies commissioned by CRC to evaluate the capability of several approaches for determining the heat of vaporization (HOV) of gasoline-like fuels. The "complete" HOV is the energy required to completely convert a given quantity of a substance from a liquid to a gaseous state at a given temperature and pressure. Accurate HOV information is needed for determining engine charge cooling effects, heat balances, efficiency, and design and for a comparison of the performance of various fuels. Prior to the current study, no validated approaches existed for measuring the HOVs of multi-component mixtures such as gasoline, although estimated values appear in the literature. The traditional Clausius-Clapeyron approach for determining the HOV of pure components from the slope of the natural logarithm of vapor pressure vs 1/T plot does not rigorously apply for multi-component mixtures.

One study conducted by Bob McCormick, Gina Fioroni, and Lisa Fouts of NREL evaluated Thermal Gravimetric Analysis-Differential Scanning Calorimetry (TGA-DSC) and compared the results to calculated values obtained by summing the products of the individual component HOVs multiplied by their concentrations as determined by Gas Chromatographic Detailed Hydrocarbon Analyses (DHA). Another study conducted by Steve Sauerbrunn of the University of Delaware also evaluated a TGA-DSC approach. The report written by NREL appears first, followed by the report written by Sauerbrunn.

The techniques were first validated by measuring the HOVs of pure components and comparing to literature values. They were then applied to measure the "complete" HOVs of three of the FACE[1] Gasolines (A, D, & H) and blends of FACE A and H with nominally 10, 15, and 30 vol. % ethanol. The FACE Gasolines is a research matrix built around the parameters of octane (RON and octane sensitivity) and fuel chemistry (aromatics and n-paraffins content) that was designed by CRC's FACE Working Group and subsequently blended and offered for sale by ChevronPhillips Chemical Co.

The average HOV results for the FACE Gasolines and the blends with ethanol are summarized in the table below. The results from both the NREL and U. Delaware studies are very close and indicate that TGA-DSC can be used to measure the HOVs of gasoline-like fuels. The NREL studies additionally indicate that the DHA-based computational method provides results very similar to those measured in TGA-DSC (generally within 10% or less).

A future phase of the work will focus on further validating the approaches by measuring the "complete" HOVs of several fuel boiling range market gasolines and extending the effort to measurement of the fractional or partial heats of vaporization that are applicable to cold-start and transient conditions in engines.

[1]Fuels for Advanced Combustion Engines (FACE)

Summary of Average "Complete" Heats of Vaporization (HOV)

Sample	"Complete" Heat of Vaporization (kJ/kg)		
	NREL		U. Delaware
	DHA	TGA-DSC	TGA-DSC
Isooctane		324	323
Toluene		415	420
Ethanol		936	
FACE Gasoline A	327	380	346
FACE A + 10% EtOH	386	410	402
FACE A + 15% EtOH	417	454	439
FACE A + 30% EtOH	507	543	540
FACE Gasoline D	349	354	364
FACE Gasoline H	367	396	383
FACE H + 10% EtOH	423	454	408
FACE H + 15% EtOH	453	488	434
FACE H + 30% EtOH	541	574	603

Measurement of Heat of Vaporization of Gasoline-Ethanol Blends by Detailed Hydrocarbon Analysis and Differential Scanning Calorimetry Coupled to Thermogravimetric Analysis

CRC Project: AVFL-27, Phase 1

Part A

Gina M. Fioroni, Lisa Fouts, Robert L. McCormick

National Renewable Energy Laboratory

April 2016

Table of Contents

List of Figures and Tables: ii

List of Acronyms ii

Executive Summary iii

Background 1

Approach 2

Samples Tested: 2

Blend Preparation: 2

Detailed Hydrocarbon Analysis: 2

Differential Scanning Calorimetry/Thermogravimetric Analysis: 3

Results and Discussion 5

Pure Component Results: 5

Experimental Determination of Ethanol Blend Level: 5

Heat of Vaporization and Detailed Hydrocarbon Analysis Results: 5

Previous Heat of Vaporization Results on Gasoline Ethanol Blends: 6

Heat of Vaporization versus Fraction Evaporated: 7

Instability in Thermograms for Fuel H: 13

Sample Loss Due to Evaporation: 13

Residual Sample Remaining: 13

Conclusions 15

List of References 16

Appendices 17

DHA Data: 17

Thermograms for all sample runs: 22

List of Figures and Tables:

Figure 1: Example Chromatogram for the DHA Analysis 3
Figure 2: Typical Thermogram from DSC/TGA Run 4
Table 1: Pure Component HOV Results by DSC/TGA 5
Table 2: D5501 Results for Blends Prepared at NREL 5
Table 3: HOV results for gasoline and gasoline-ethanol blends by DHA and DSC/TGA 6
Figure 3: HOV Results from SAE 2015-01-0763 Compared to CRC AVFL-27 Samples 7
Figure 4: Cumulative HOV per total sample mass as a function of fraction evaporated for FACE A and FACE A Blends. 9
Figure 5: Cumulative HOV per total sample mass as a function of fraction evaporated for FACE H and FACE H Blends. 9
Figure 6: Cumulative HOV per total sample mass as a function of the fraction evaporated for FACE A, D, and H. 9
Figure 7. Cumulative HOV per evaporated sample mass as a function of fraction evaporated for FACE A and FACE A Blends 10
Figure 8. Cumulative HOV per evaporated sample mass as a function of fraction evaporated for FACE H and FACE H Blends. 10
Figure 9. Replicate results for all FACE A blends showing mass loss rate, instantaneous HOV, and cumulative HOV. 11
Figure 10. Replicate results for all FACE H blends showing mass loss rate, instantaneous HOV, and cumulative HOV. 12
Table 4: Residual Sample Mass for Each Sample Run 14

List of Acronyms

CP:	Common abbreviation for Clausius-Clapeyron equation
CRC:	Coordinating Research Council
DHA:	Detailed Hydrocarbon Analysis
DI:	Direct Injection
DSC/TGA:	Differential Scanning Calorimetry/Thermal Gravimetric Calorimetry
Exx:	Blend of ethanol and gasoline containing xx vol% ethanol
FACE:	Fuels for Advanced Combustion Engines
FID:	Flame Ionization Detector
GC:	Gas Chromatography
HOV:	Heat of Vaporization
NREL:	National Renewable Energy Laboratory

Executive Summary

The objective of this study was to develop a method(s) to measure the Heat of Vaporization (HOV) of gasoline and gasoline and ethanol blends. Both calculation of HOV from a Detailed Hydrocarbon Analysis (DHA) and direct measurement by Differential Scanning Calorimetry coupled to Thermogravimetric Analysis (DSC/TGA) were used.

Three base gasoline fuels were supplied to NREL from CRC. Fuels for Advanced Combustion Engines (FACE) gasolines A and H were blended by NREL with ethanol at the E10, E15, and E30 levels. FACE gasoline D was also tested without ethanol. Samples were analyzed by DSC/TGA in duplicate, in a randomized order. The base FACE fuels were analyzed by DHA and these analyses were adjusted for ethanol content in the blends to calculate HOV at each blend level from the HOV of the individual components. Additionally, the HOV of isooctane was measured by DSC/TGA and compared to literature values in order to determine the accuracy of the method.

Both the DSC/TGA and DHA provide reliable methods for the measurement of HOV of complex mixtures. Analysis of several pure components using the DSC/TGA demonstrates the accuracy of this method with values matching closely to those reported in the literature. For several blend levels and various base gasolines, the HOV measured by the DSC/TGA agrees well with those measured by DHA. Curves of mass loss rate versus fraction evaporated show a sharp drop in mass loss rates for ethanol blends, which occurs at higher fraction evaporated with increasing ethanol content. We speculate that this drop in mass loss rate occurs at the same point in the sample evaporation as the end of the well-known T50 plateau in the distillation curve of ethanol-gasoline blends.

While reliable measurements of total HOV can be obtained, a detailed analysis of the DSC/TGA data revealed a number of issues with the current NREL experimental setup that make measurements of instantaneous or cumulative HOV exhibit high experimental error. These include location of the instrument in a place where it is prone to building and other random vibrations, as well as difficulty in fully replicating the start of the experiment such that initial HOV values at low mass fraction evaporated are not reliable. Relocation of the instrument and a method development program to address these issues is recommended.

Background

Octane number is a measure of a fuel's tendency to autoignite. Autoignition of a fuel can cause a spark-ignited engine to knock. Ethanol is commonly blended into gasoline to increase a fuel's knock resistance. Additionally, ethanol may also provide a knock resistance advantage for direct injection (DI) engines by providing an evaporative cooling effect upon injection. This cooling effect can be quantified as the heat of vaporization (HOV).

The measurement of HOV for pure components is relatively straightforward and is done by measuring the vapor pressure of the component of interest at various temperatures. The Clausius-Clapeyron (CP) equation (Equation 1) is then used to calculate the HOV:

$$\ln[P_{T1,vap}/P_{T2,vap}] = (\Delta H_{vap}/R)[1/T_2 - 1/T_1] \quad [1]$$

where :

P= vapor pressure

T=temperature (K)

ΔH_{vap} =heat of vaporization (J/mol)

R = ideal gas constant

For fuel mixtures, the vapor pressure is mostly determined by the low molecular weight components in the fuel which biases the HOV result calculated by the CP equation on the low side. We have previously reported on the use of differential scanning calorimetry/thermogravimetric analysis (DSC/TGA) and detailed hydrocarbon analysis (DHA) for estimation of gasoline HOV.[1] To our knowledge, a straight-forward and rapid measurement of the HOV of mixtures, especially blends of ethanol in gasoline, has not previously been developed. Here we apply these methods to a broader range of gasolines and develop more critical approaches to data analysis and estimation of experimental error.

Approach

Samples Tested:

Three FACE gasolines (A, D, and H) were supplied to NREL by CRC. Detailed characterization of the FACE gasolines by CRC's FACE Working Group has been reported.[2] Two of the base gasolines were blended with reagent grade ethanol to create an E10, E15, and E30. All of these samples were to be tested by DSC/TGA in duplicate in a randomized order. All three of the base gasoline compositions were measured by DHA. The samples prepared and evaluated are listed below.

1. FACE Gasoline A
2. FACE Gasoline A + 10 vol% Ethanol
3. FACE Gasoline A + 15 vol% Ethanol
4. FACE Gasoline A + 30 vol% Ethanol
5. FACE Gasoline H
6. FACE Gasoline H + 10 vol% Ethanol
7. FACE Gasoline H + 15 vol% Ethanol
8. FACE Gasoline H + 30 vol% Ethanol
9. FACE Gasoline D

Additionally, HOV was measured for reagent grade isooctane, a typical gasoline boiling-range component, by DSC/TGA to ensure accuracy of the method.

Blend Preparation:

Blends were prepared using FACE A and H gasolines with reagent grade 200 proof ethanol purchased from Pharmco-AAPER. Blending was conducted with cold liquids taken from a freezer to reduce evaporation of the light components. The blendstocks were volumetrically measured, splash blended, and mixed by hand to ensure homogeneity. Samples were stored in a freezer (approximately -18°C) and care was taken to reduce the headspace in the storage containers. Actual ethanol blend content was validated by ASTM D5501 and adjusted for the amount of water present as measured by Karl Fischer (D6304).

Detailed Hydrocarbon Analysis:

DHA was measured using method D6729. Briefly, the sample is analyzed by gas chromatography utilizing a flame ionization detector (GC-FID), which provides a list of components and their concentrations. Components are then identified by comparing this list to a certified hydrocarbon standard purchased from Separation Systems (Gulf Breeze, FL). An example chromatogram is shown in Figure 1. Detailed tables of results for all three FACE base gasolines are included in the Appendix.

Using the individual component critical properties, the HOV in kJ/mole for each individual component is calculated using the Pitzer acentric factor correlation, as described in Reid, Prausnitz, and Poling[3] (Equation 2):

$$\frac{HOV}{RT_c} = 7.08(1 - T_r)^{0.354} + 10.95\omega(1 - T_r)^{0.456} \qquad [2]$$

where:

HOV = heat of vaporization

R= gas constant,0.008314 kJ/mol K

T_c = critical temperature

T = desired temperature

T_r =reduced temperature, T/T_c

ω =acentric factor

Critical temperature and acentric factor for individual compounds were taken from literature sources.[4,5] The individual component HOV (HOVi) values are then multiplied by their mole fraction and summed to yield a total HOV for the mixture. Components less than 0.05 mol% in concentration were eliminated from the list (typically about 1-3 mol% of the total sample). All calculations were performed at 25°C, but an advantage of this method is that the HOV can easily be calculated at any temperature. In contrast, while DSC/TGA measurements are possible in theory at any temperature, temperatures above 25°C are challenging because of the difficulty in loading a highly volatile gasoline sample into the instrument without experiencing high levels of sample loss prior to experiment initiation.

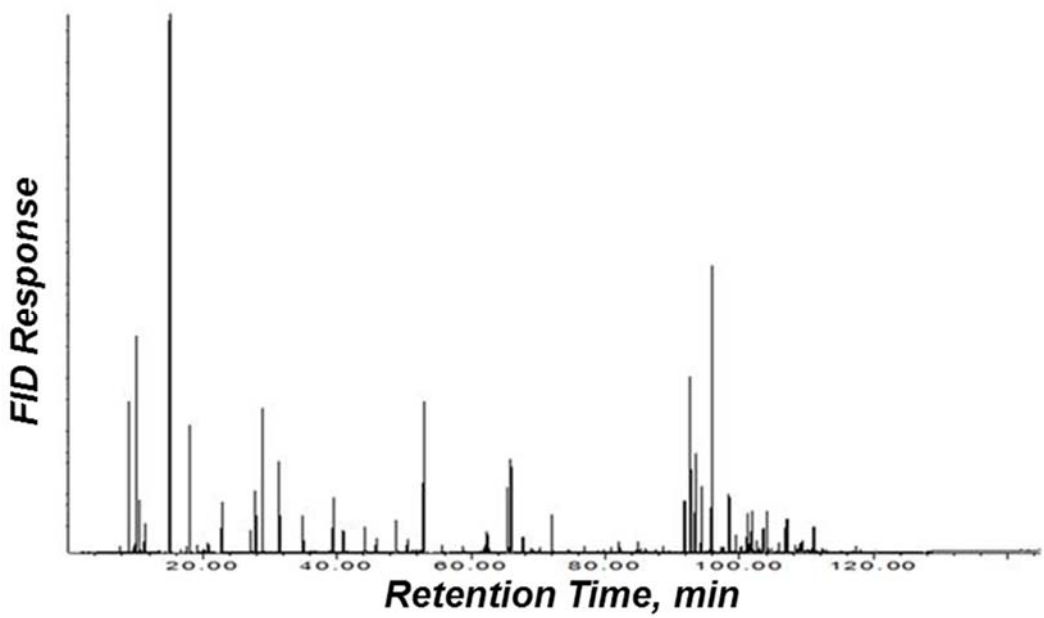

Figure 1: Example Chromatogram for the DHA Analysis

After initial characterization of the base fuel, calculating HOV of blends with ethanol is done by combining the base gasoline HOV with the HOV contribution from ethanol. The ethanol HOV of 924 kJ/kg was multiplied by the weight fraction ethanol in the sample to get the HOV value for the amount of ethanol present. The HOV of the base FACE gasoline was adjusted for the ethanol by subtracting the percent ethanol from 100% and multiplying this number by the HOV calculated for the FACE gasoline. The two values were then summed to get a total HOV value for each blend.

Differential Scanning Calorimetry/Thermogravimetric Analysis:

DSC/TGA allows direct and rapid measurement of total HOV as well as HOV as a function of the fraction evaporated. For DSC/TGA, all samples were measured in duplicate and in a randomized order.

A TA Instruments Q600 SDT was used for HOV measurements. The instrument was calibrated to manufacturer's specifications and the cell constant was further calibrated with three replicate HOV

measurements for deionized water (coefficient of variation 1.6%). The ratio of the average of the three water runs to the literature value of water (2441 J/g)[6] was used to generate a correction factor of 0.9435 which was used to correct all measured values. Note that in our previous study we inadvertently used the HOV of water at its boiling point,[1] using the correct value at 25°C increases the measured values by 7 to 9%.

Aluminum sample pans with a maximum 90 µL capacity were used for the analysis (Mettler, part# ME-51119872). In order to reduce the amount of sample loss prior to the instrument starting data collection, a lid with a 75 µm laser-drilled hole (TA Instruments, part# 900860.901) is placed on top of the sample pan. At 23°C, the instrument was zeroed by taring a reference pan against an empty sample pan. Thirty µL (~23 mg) of a sample that had been held on dry ice is immediately transferred to the sample pan via a gas- tight microliter syringe and the lid is placed on top. The instrument program is set to have no nitrogen flow on during sample introduction into the test cell. Once the test cell is closed, the nitrogen flow is increased to 50 mL/min after 6 seconds and the instrument is held isothermally at 23°C for the duration of the test. The heat flow and the sample mass loss are measured simultaneously throughout the experiment and heat flow, weight loss, and the derivative of weight loss are plotted. The HOV is calculated by subtracting the zero heat flow (heat flow in empty pans) from the total heat flow at each point. The trapezoid method is then used to determine the area under the curve which is then divided by the mass of the sample to give the total HOV. Figure 2 shows a typical thermogram from a sample run. Samples typically take 1-2 hours to run to completion. For pure components, the HOV can also be calculated by dividing the heat flow by the derivative of weight loss and averaging these values. This is only possible with pure components which evaporate monotonically. Thermograms for all fuels and components tested are included in the Appendix.

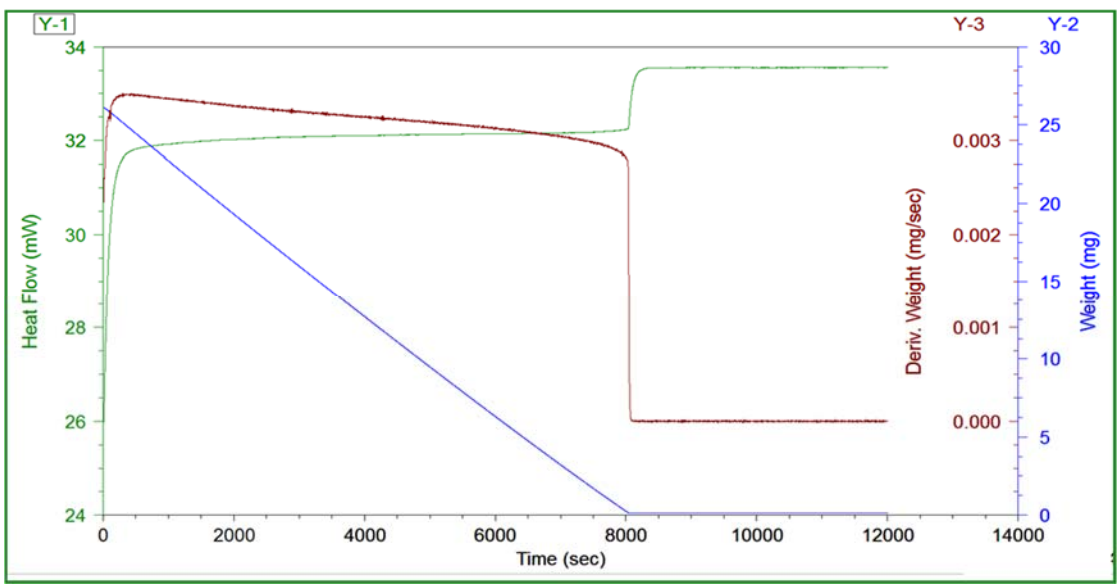

Figure 2: Typical Thermogram from DSC/TGA Run

Results and Discussion

Results for Isooctane:

In order to test the accuracy of our method the HOV of isooctane was measured by the DSC/TGA method. Table 1 also reports results of two new replicate runs for isooctane. The difference between these replicates is 3.7%, and their average value of 324.2 kJ/kg differs from the literature value by 5.1%.

Table 1: Pure Component HOV Results by DSC/TGA

Compound	Literature (kJ/kg)[7]	Total Area (kJ/kg)	% Difference
Isooctane	308.0	330.1	6.9
Isooctane	308.0	318.2	3.3

Experimental Determination of Ethanol Blend Level:

Analysis was by the ASTM D5501 method. A calibration curve was prepared and run for quantitation and the daily check standard was used to verify proper calibration. The check standard was within 0.1% difference of the certificate of analysis value. Table 2 shows that all of the samples were blended accurately.

Table 2: D5501 Results for Blends Prepared at NREL

Sample	Vol % Ethanol	Wt % Ethanol	Mol % Ethanol
FACE A E10	9.79	11.15	21.32
FACE A E15	14.96	16.91	30.52
FACE A E30	30.06	33.23	51.80
FACE H E10	10.08	10.41	19.74
FACE H E15	15.41	15.89	28.57
FACE H E30	31.21	32.00	49.91

Heat of Vaporization and Detailed Hydrocarbon Analysis Results:

Table 3 shows the results of both the DHA and DSC/TGA for the gasolines and blends. The literature value of 924.0 kJ/kg[7] for the HOV of ethanol was used in these calculations. Between duplicate sample runs the highest difference was 2.2%, demonstrating good method repeatability. In comparing the DHA results versus the DSC/TGA runs, the DSC/TGA results are always higher, on average by about 7%. Also notable is that HOV derived from DHA for FACE gasoline D measured by NREL (349.4 kJ/kg) was indistinguishable from HOV derived from DHA measured by Chevron as part of CRC's FACE Working Group (348.1 kJ/kg). Both methods are potentially subject to systematic errors. These include sample loss by evaporation prior to initiating the measurement for DSC/TGA, and errors in quantification and in estimating pure component HOV from equation 2 for DHA. Thus it is difficult to make an assessment of which method provides the more accurate result at the present time.

Table 3: HOV results for gasoline and gasoline-ethanol blends by DHA and DSC/TGA

Sample	DSC/TGA (kJ/kg)	Average (kJ/kg)	% diff Replicates	DHA (kJ/kg)*	% diff DHA vs DSC/TGA
A	380.5				
	379.3	379.9	0.3	327.3	14.9
A E10	410.2				
	409.4	409.8	0.2	385.7	6.1
A E15	458.8				
	449.3	454.05	2.1	416.6	8.6
A E30	537.1				
	548.8	542.95	-2.2	506.7	6.9
D	354.6				
	352.7	353.65	0.5	349.4	1.2
H	398.6				
	392.7	395.65	1.5	366.8	7.6
H E10	455.4				
	453.2	454.3	0.5	423.0	7.1
H E15	491.1				
	484.5	487.8	1.4	452.7	7.5
H E30	573.8				
	573.2	573.5	0.1	540.7	5.9

*Mole percent excluded from the DHA calculation for components present at less than 0.05 mol%: FACE A 0.97, FACE D 1.03, FACE H 4.07.

Previous Heat of Vaporization Results on Gasoline Ethanol Blends:

In previous work, NREL ran several other gasoline/ethanol blends by both DHA and DSC/TGA with the results being published in a SAE paper.[1] These samples were prepared using a winter conventional blendstock for oxygenate blending (CBOB) and a California Air Resources Board reformulated blendstock for oxygenate blending (CARBOB) blended with 200 proof ethanol. A comparison of previous results with data obtained from the samples in this study (Figure 3) shows that the DSC/TGA and DHA results for the FACE gasolines compare well with results for the CBOB and CARBOB blends – although the DSC/TGA values for the FACE gasolines trend higher because of the improved instrument calibration used here. Additionally, it can be seen that ethanol has a much more significant impact on the HOV than variations in base fuel components. The HOV differences between the different base fuels show a range of, at most 75 kJ/kg, while addition of just 20% ethanol to a given base fuel increases the HOV by over 100 kJ/kg.

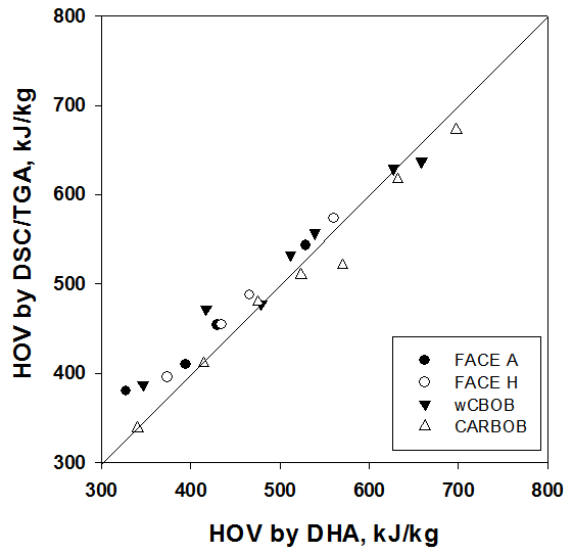

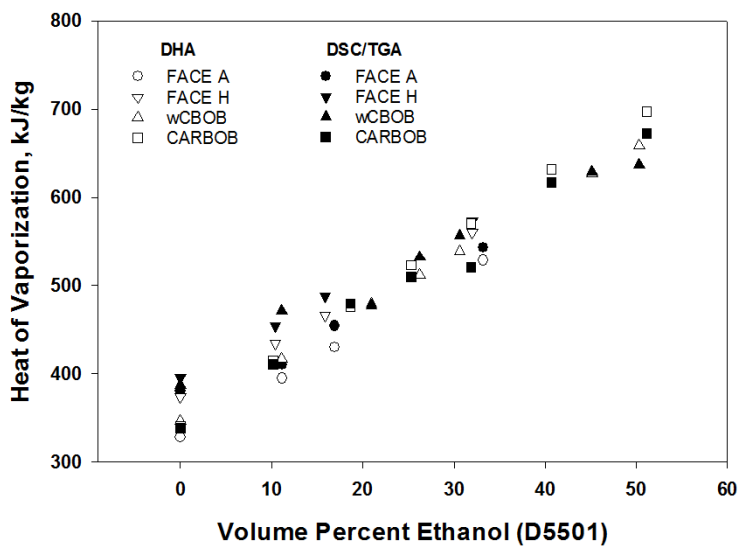

Figure 3: HOV Results from SAE 2015-01-0763 Compared to CRC AVFL-27 Samples

Heat of Vaporization versus Fraction Evaporated:

An additional parameter that can be evaluated using the DSC/TGA method is the analysis of the HOV as a function of the fraction evaporated. In reference 1 we calculated the HOV per total mass of sample versus fraction evaporated, as shown here in Figures 4, 5 and 6 for the FACE A and H gasolines and their blends, and FACE gasoline D. Unlike distillation curves where there is a flattening of the curve while the ethanol evaporates from the sample, cumulative HOV increases monotonically as the fuel evaporates.

A potentially more informative way to analyze the data is as cumulative HOV per evaporated sample mass versus fraction evaporated (in this test a pure compound would yield a constant value of the HOV at any percent evaporated). Results of this analysis for the FACE A and H blends are shown in Figures 7 and 8. These charts reveal significant variation in the measured HOV at mass fraction evaporated below 0.1, likely because of the challenges of loading a highly volatile sample into the DSC/TGA instrument and

initiating the experiment in a repeatable way. However, some of the differences between samples are repeatable. For example, FACE H E15 shows a much lower initial cumulative HOV in Figure 8 than would be expected based on results for the corresponding E10 and E30 blends. However, a replicate of this experiment on a different day yielded very similar results, as did a third replicate on a freshly prepared sample. Thus a combination of experimental methodology and fuel property factors may be responsible for the variable results. Nevertheless, in terms of total HOV of the sample, the DSC/TGA method appears to produce a reasonable and repeatable result.

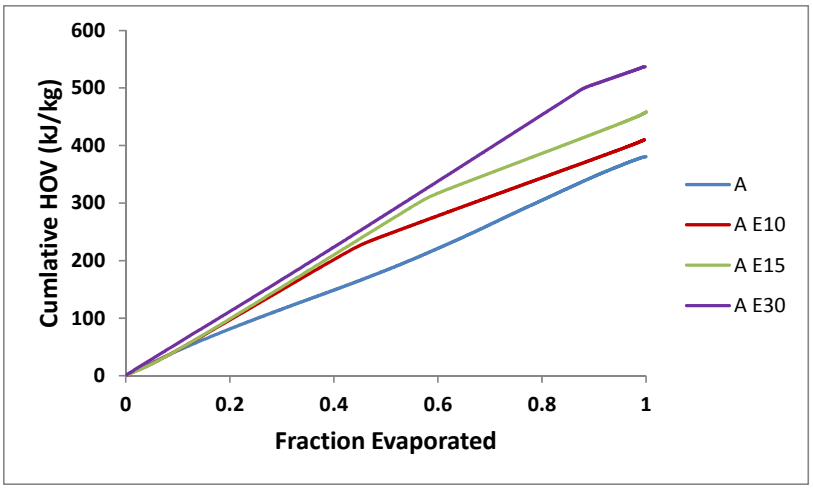

Figure 4: Cumulative HOV per total sample mass as a function of fraction evaporated for FACE A and FACE A Blends.

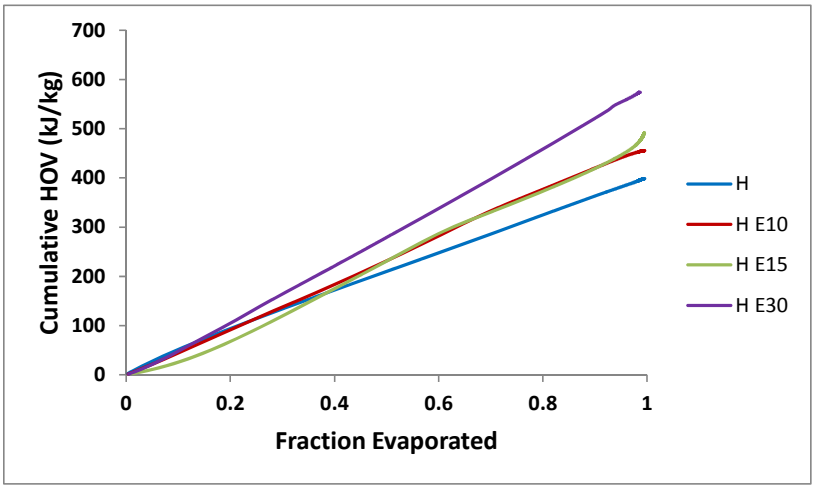

Figure 5: Cumulative HOV per total sample mass as a function of fraction evaporated for FACE H and FACE H Blends.

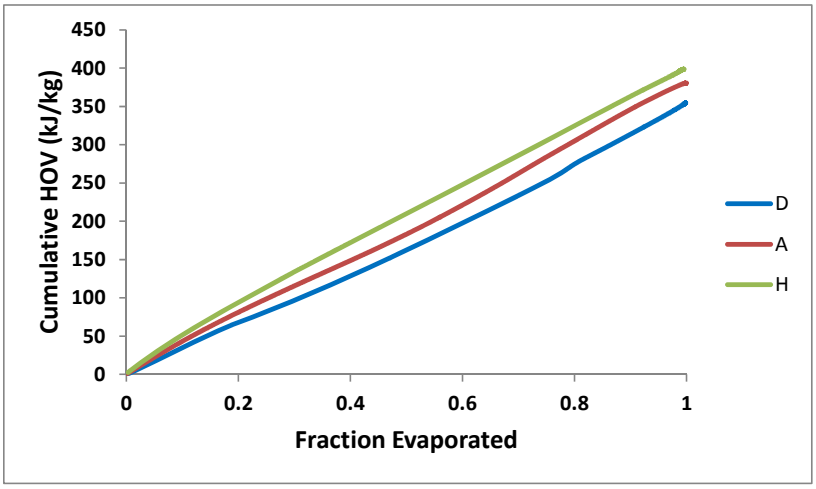

Figure 6: Cumulative HOV per total sample mass as a function of the fraction evaporated for FACE A, D, and H.

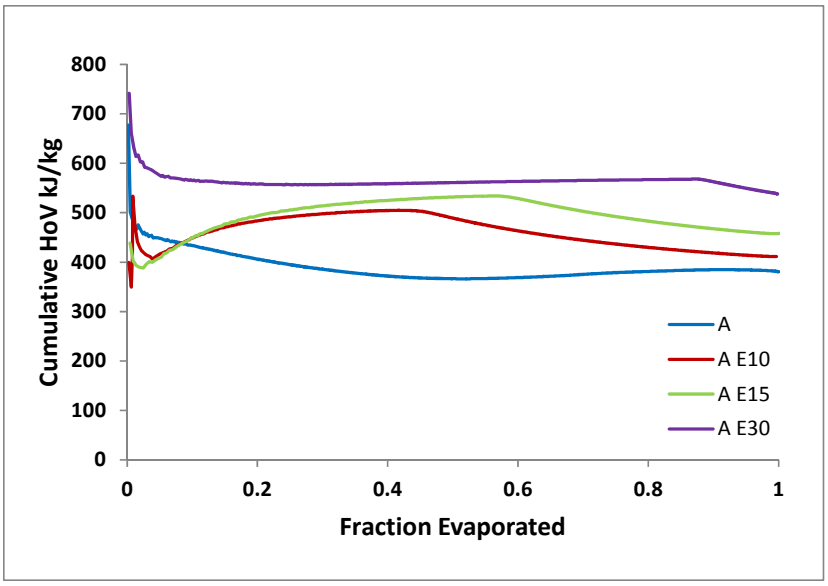

Figure 7. Cumulative HOV per evaporated sample mass as a function of fraction evaporated for FACE A and FACE A Blends

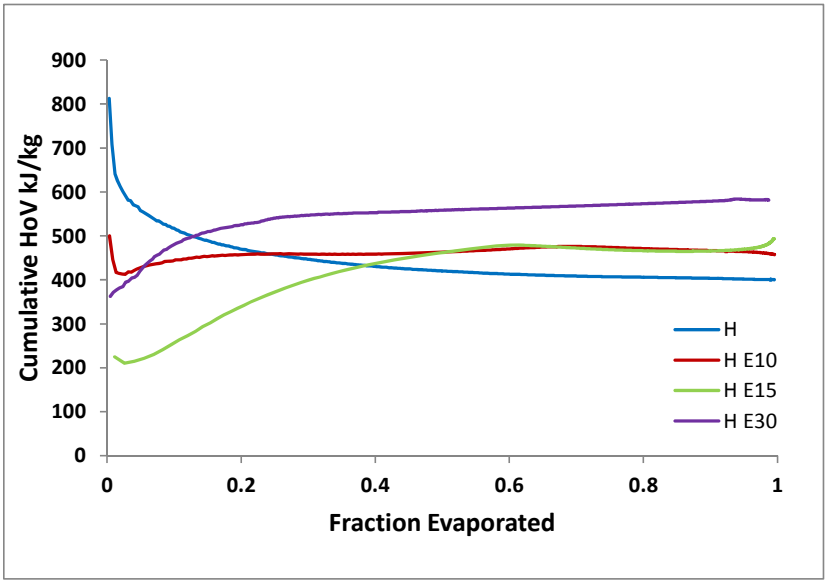

Figure 8. Cumulative HOV per evaporated sample mass as a function of fraction evaporated for FACE H and FACE H Blends.

Figures 9 and 10 show cumulative HOV per evaporated mass, instantaneous HOV, and rate of mass loss for all replicate experiments performed on the FACE A and H blends. Instantaneous HOV is the measured instantaneous baseline corrected heat flow (mJ/s) divided by the measured rate of mass loss (mg/s). These charts reveal a number of interesting observations. While comparison between replicates shows overall consistency, there are also a number of unreplicated spikes or dips in the curves. We believe that these are caused by the non-optimal location of the DSC/TGA instrument where it is susceptible to building vibrations from HVAC equipment, closing of doors, or the table being bumped by a person. For future experiments it is recommended that this instrument be moved to a better location.

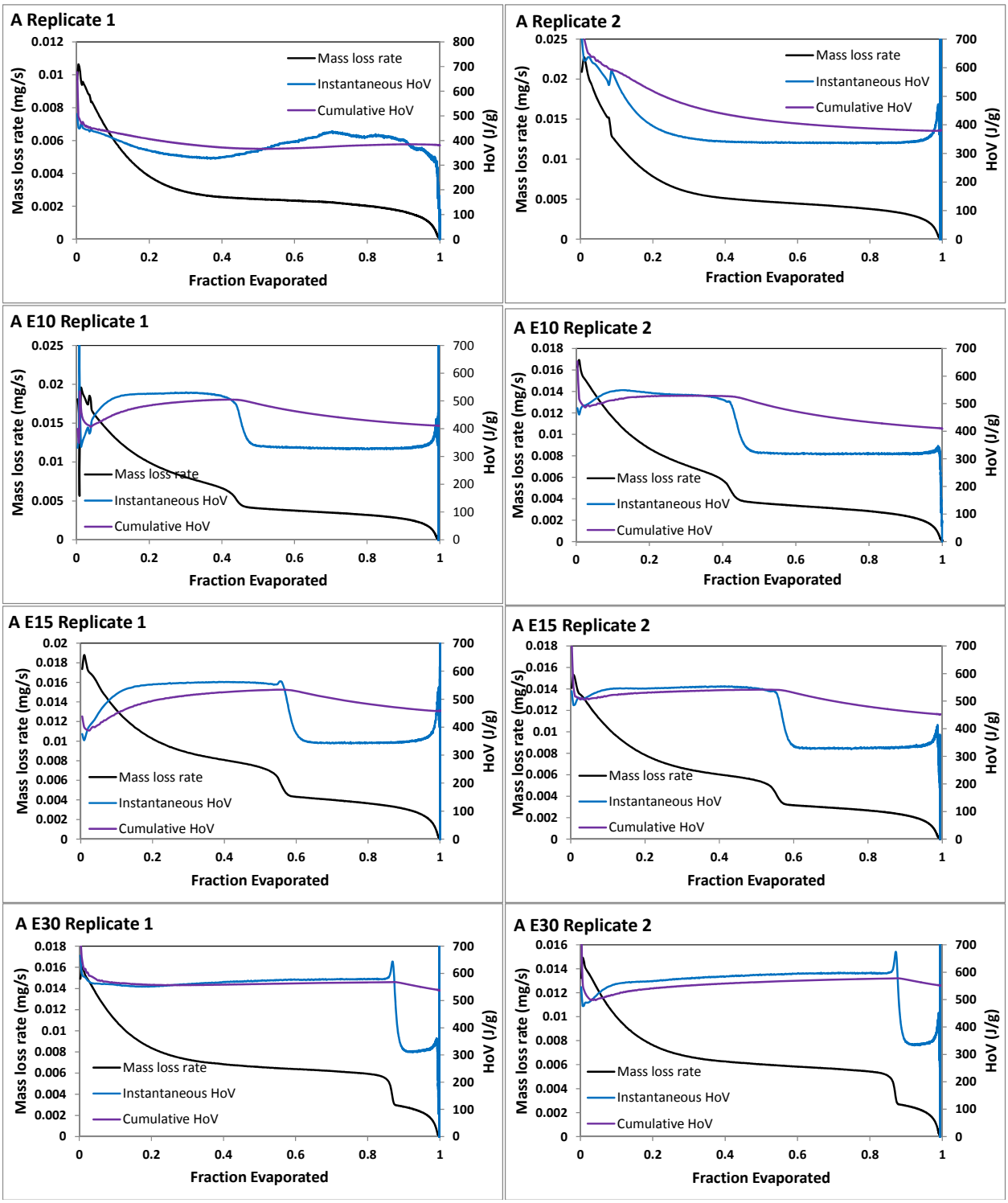

Figure 9. Replicate results for all FACE A blends showing mass loss rate, instantaneous HOV, and cumulative HOV.

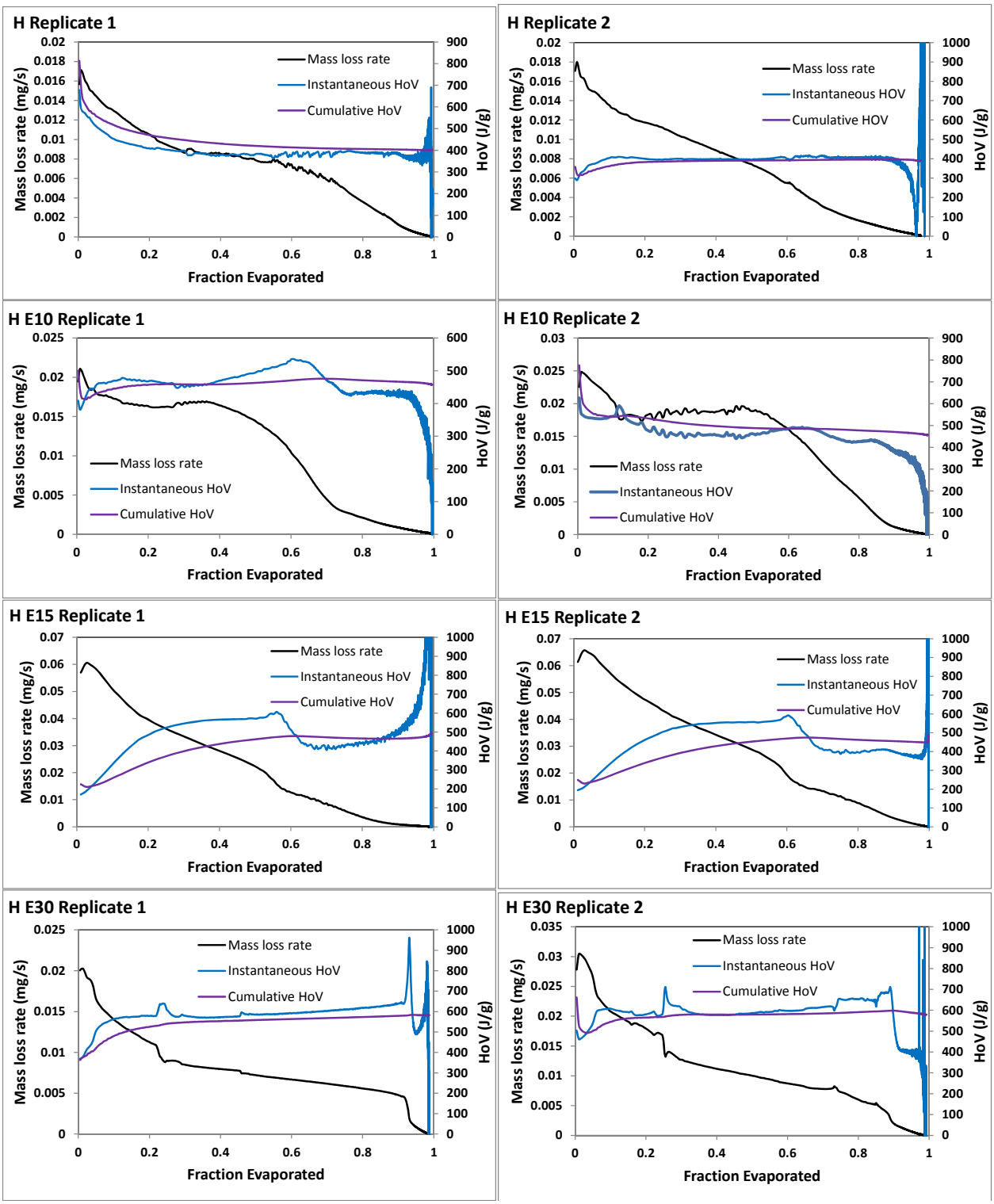

Figure 10. Replicate results for all FACE H blends showing mass loss rate, instantaneous HOV, and cumulative HOV.

The mass loss rates in Figures 9 and 10 also show important features that are replicated. For the FACE A ethanol blends there is a sharp dip in mass loss rate at about 0.45 fraction evaporated for E10, 0.55 for E15, and 0.85 for E30. A similar dip in mass loss rate is observed for the FACE H E15 and E30 blends. We speculate that this occurs at the same point as the end of the well-known plateau or flattening in the distillation curve for ethanol gasoline blends. CRC Report AVFL-24 reports D86 distillation results for the FACE gasolines and ethanol blends containing 10, 15, and 30 vol% ethanol.[2] There is good correlation between the mass fraction evaporated at the mass loss dip and the volume fraction evaporated at the end of the distillation plateau for FACE A (0.4, 0.5, and 0.8 vol fraction for E10, E15, and E30, respectively). This correspondence is not observed for the FACE H ethanol blends.

Instability in Thermograms for Fuel H:

Mass loss rates and instantaneous HOV curves for FACE A in Figure 9 typically show smooth curves with little indication of instability or random variation (other than that noted above). For Fuel H and ethanol blends produced from it, the curves in Figure 10 show significant instability in many cases (saw-tooth or non-smooth variation of the curve). If we had only observed this for one sample we would likely have ignored it, but it is common to most tests with Fuel H blends. Based on published data on the properties of the FACE gasolines, Fuel H is relatively high boiling within the context of the FACE gasolines (relatively high T90 of 164°C and endpoint of 209°C – highest endpoint of the FACE gasolines) and high aromatic content (35.3 vol% by FIA).[2] As shown in Table 3, DSC/TGA and DHA give values of HOV for FACE H that differ by only 0.9%, so this instability does not seem to affect the repeatability of the HOV measurement. This is a notable feature of the data that we cannot at this time explain.

Sample Loss Due to Evaporation:

A concern with measuring the HOV using DSC/TGA is potential sample loss due to evaporation prior to the start of data acquisition. Two methods were used to determine how much sample was lost prior to starting the test. In one, the sample syringe was weighed before and after the sample was transferred into the sample pan. The weight injected by the syringe was compared to the starting weight recorded by the instrument. We chose one sample, A E10 for this test and recorded the weight before and after for five replicates. The average sample loss over the five replicates was 1.7 mg which corresponds to 7.1% of the sample. The second method used was to place a pan on the balance, inject the sample into the pan and record the weight lost every 10 seconds for a full minute.[1] It typically takes 30 seconds or less to load the sample into the instrument, so the average sample loss at 30 seconds was used to calculate the percent of sample lost and it was found to be 5% or less. The two methods for determining sample loss are essentially equivalent.

Residual Sample Remaining:

The amount of sample remaining in the pan at the end of the test, or residual mass, was noted for each sample. Note that this was not taken into account in any way in calculation of the measured HOV result. The residual mass was typically 0.1 mg or less, with the exception of base fuel H E30 blends where the residue was between 0.2 and 0.3 mg. This corresponds to an average of 0.43% of the starting sample mass (or an average of 0.9% for base Fuel H) remaining at the conclusion of the test. We attribute this to the fact that base fuel H contained the highest amount of heavier weight components, based on the DHA, compared to FACE fuels A and D. Table 4 shows the residual amount of sample remaining in mg for each test. Even though some samples had more mass remaining than others, it appears that the sample measurement was quite repeatable and the remaining sample in the pan had only a small effect on the total HOV measured.

Table 4: Residual Sample Mass for Each Sample Run

Sample	Residual Mass, mg
Isooctane 1	-0.018
Isooctane 2	-0.002
FACE A 1	-0.0006
FACE A 2	0.1048
A E10 1	0.09068
A E10 2	0.0006
A E15 1	-0.0005
A E15 2	0.1076
A E30 1	0.03457
A E30 2	0.1121
FACE D 1	0.06051
FACE D 2	0.00061
FACE H 1	0.09569
FACE H 2	0.1348
H E10 1	0.09819
H E10 2	0.1109
H E15 1	0.1016
H E15 2	0.02126
H E30 1	0.2788
H E30 2	0.2221

Conclusions

Both the DSC/TGA and DHA provide reliable methods for the measurement of HOV of complex mixtures. Analysis of several pure components using the DSC/TGA demonstrates the accuracy of this method with values matching closely to those reported in the literature. For several blend levels and various base gasolines, the HOV measured by the DSC/TGA agrees well with those measured by DHA. Curves of mass loss rate versus fraction evaporated show a sharp drop in mass loss rates for ethanol blends, which occurs at higher fraction evaporated with increasing ethanol content. We speculate that this drop in mass loss rate occurs at the same point in the sample evaporation as the end of the well-known T50 plateau in the distillation curve of ethanol-gasoline blends.

While reliable measurements of total HOV can be obtained, a detailed analysis of the DSC/TGA data revealed a number of issues with the current experimental setup that cause high uncertainty for measurements of instantaneous or cumulative HOV, especially at low fraction evaporated. These include location of the instrument in a place where it is subject to building and other random vibrations, as well as difficulty in fully replicating the start of the experiment such that initial HOV values at low mass fraction evaporated are not reliable. Relocation of the instrument and a method development program to address these issues are recommended.

List of References

1. Chupka, G.M., Christensen, E., Fouts, L., Alleman, T.L., Ratcliff, M., McCormick, R.L., "Heat of Vaporization Measurements for Ethanol Blends Up To 50 Volume Percent in Several Hydrocarbon Blendstocks and Implications for Knock in SI Engines" SAE Int. J. Fuels Lubr. 2015, doi:10.4271/2015-01-0763.
2. Cannella, W., Foster, M., Gunter, G., Leppard, W. "FACE Gasolines and Blends with Ethanol: Detailed Characterization of Physical and Chemical Properties" CRC Report No. AVFL-24, July 2014.
3. Reid, R.C., Prausnitz, J.M., and Poling, B.E. *The Properties of Gases and Liquids*, 4th ed., McGraw-Hill, New York, 1987.
4. API Technical Databook – Petroleum Refining, API, 1993.
5. Yaws, C.L., *Yaws' Handbook of Thermodynamic and Physical Properties of Chemical Compounds: Physical, Thermodynamic and Transport Properties for 5,000 Organic Chemical Compounds*. McGraw-Hill, New York, 2003.
6. Marsh, K. N., Ed., *Recommended Reference Materials for the Realization of Physicochemical Properties,* Blackwell, Oxford, 1987.
7. http://webbook.nist.gov/chemistry/ accessed November 2015.

Appendices

DHA Data:

FACE A:

TIME	COMPONENT	%MOL	Tc, K	Accentric Factor	Tr	HOV (kJ/kg)	HOVi (kJ/kg)	MW Gasoline (g/mol)	HOV total (kJ/Kg)
8.77	i-Butane	0.307	407.85	0.1770	0.7	18.69	5.75	99.5	327.3
9.92	n-Butane	5.359	425.16	0.1931	0.7	20.63	110.53		
14.74	i-Pentane	14.073	460.43	0.2275	0.6	24.66	347.08		
17.68	n-Pentane	0.063	469.71	0.2486	0.6	26.07	1.65		
22.42	2,2-Dimethylbutane	0.087	488.78	0.2339	0.6	27.39	2.37		
26.68	Cyclopentane	0.067	511.76	0.1943	0.6	28.19	1.88		
27.35	2,3-Dimethylbutane	1.864	499.98	0.25	0.6	28.80	53.67		
28.37	2-Methylpentane	2.101	497.50	0.28	0.6	29.49	61.95		
30.87	3-Methylpentane	0.808	504.43	0.28	0.6	30.11	24.34		
40.37	2,4-Dimethylpentane	3.049	519.79	0.30	0.6	32.31	98.51		
45.00	2-Methyl-c-hexene-3	0.385	528.96	0.31	0.6	33.52	12.91		
48.25	2-Methylhexane	12.693	530.37	0.33	0.6	34.18	433.82		
49.94	3-Methylhexane	6.627	535.25	0.32	0.6	34.43	228.13		
50.68	1t,3-Dimethylcyclopentane	0.303	553.15	0.27	0.5	34.23	10.37		
51.22	1c,3-Dimethylcyclopentane	0.319	550.93	0.27	0.5	34.24	10.94		
51.79	1t,2-Dimethylcyclopentane	0.369	553.15	0.27	0.5	34.30	12.66		
51.96	3-Ethylpentane	0.636	540.64	0.31	0.6	34.52	21.95		
52.50	2,2,4-Trimethylpentane	25.628	543.96	0.30	0.5	34.62	887.23		
55.11	n-Heptane	6.607	540.21	0.35	0.6	35.85	236.84		
58.17	Methylcyclohexane	0.322	572.19	0.24	0.5	34.70	11.18		
60.78	Ethylcyclopentane	0.062	569.52	0.27	0.5	35.83	2.22		
61.38	2,2,3-Trimethylpentane	0.394	563.50	0.30	0.5	36.21	14.27		
61.64	2,5-Dimethylhexane	1.349	550.00	0.36	0.5	37.09	50.03		
61.95	2,4-Dimethylhexane	1.868	553.50	0.34	0.5	36.94	69.01		
64.81	2,3,4-Trimethylpentane	6.182	566.30	0.32	0.5	37.17	229.81		
65.44	2,3,3-Trimethylpentane	4.265	573.50	0.29	0.5	36.88	157.29		
67.14	2,3-Dimethylhexane	1.677	563.40	0.35	0.5	38.03	63.79		
68.64	4-Methylheptane	0.128	561.74	0.37	0.5	38.74	4.95		
68.77	3,4-Dimethylhexane	0.122	568.80	0.34	0.5	38.22	4.67		
71.52	2,2,5-Trimethylhexane	0.673	568.05	0.36	0.5	38.83	26.14		
76.39	Cyclopentane, 1-ethyl-2-methyl	0.124	585.20	0.2520	0.5	36.47	4.54		
85.59	1,1,2-Trimethylcyclohexane	0.123	612.06	0.2670	0.5	39.42	4.86		
86.99	n-Nonane	0.077	594.64	0.44	0.5	44.58	3.45		
93.81	1-Methyl-2-ethylbenzene	0.270	637.36	0.40	0.5	47.35	12.77		
95.04	C11-Isoparaffin-2	0.050	631.76	0.51	0.5	51.46	2.59		

FACE D:

TIME	COMPONENT	%MOL	Tc, (K)	Accentric Factor	Tr	HOV (kJ/kg)	HOVi (kJ/kg)	MW gasoline (g/mol)	HOV total (KJ/Kg)
8.77	i-Butane	0.116	407.85	0.1770	0.7	18.69	2.17	102.0	349.4
9.92	n-Butane	5.829	425.16	0.1931	0.7	20.63	120.22		
14.75	i-Pentane	0.145	460.43	0.2275	0.6	24.66	3.57		
17.67	n-Pentane	13.171	469.71	0.2486	0.6	26.07	343.40		
26.69	Cyclopentane	0.071	511.76	0.1943	0.6	28.19	1.99		
34.40	n-Hexane	7.250	507.37	0.3047	0.6	31.22	226.37		
48.21	2-Methylhexane	1.030	530.37	0.3282	0.6	34.18	35.21		
49.94	3-Methylhexane	0.061	535.25	0.3216	0.6	34.43	2.10		
52.55	2,2,4-Trimethylpentane	34.132	543.96	0.3031	0.5	34.62	1181.66		
61.65	2,5-Dimethylhexane	0.143	550.00	0.3576	0.5	37.09	5.32		
61.96	2,4-Dimethylhexane	0.156	553.50	0.3436	0.5	36.94	5.76		
65.38	Toluene	12.918	591.79	0.2641	0.5	37.52	484.65		
80.46	Ethylbenzene	0.390	617.17	0.3036	0.5	41.39	16.15		
81.59	m-Xylene	1.368	617.05	0.3260	0.5	42.31	57.88		
81.73	p-Xylene	0.574	616.26	0.3259	0.5	42.23	24.25		
84.35	o-Xylene	1.688	630.37	0.3127	0.5	42.98	72.53		
88.22	i-Propylbenzene	0.240	631.15	0.3377	0.5	44.12	10.60		
91.39	n-Propylbenzene	1.085	638.38	0.3462	0.5	45.17	48.99		
92.20	1-Methyl-3-ethylbenzene	2.863	637.15	0.3221	0.5	44.01	126.02		
92.39	1-Methyl-4-ethylbenzene	1.293	640.15	0.3242	0.5	44.38	57.39		
92.98	1,3,5-Trimethylbenzene	1.534	637.36	0.3985	0.5	47.35	72.63		
93.93	1-Methyl-2-ethylbenzene	1.253	637.36	0.3985	0.5	47.35	59.35		
94.58	3-Methylnonane	0.052	613.70	0.4565	0.5	47.38	2.48		
95.46	1,2,4-Trimethylbenzene	5.524	649.13	0.3792	0.5	47.66	263.28		
96.92	i-Butylbenzene	0.109	650.15	0.3811	0.5	47.85	5.20		
97.18	sec-Butylbenzene	0.112	664.54	0.2756	0.4	44.39	4.97		
97.26	n-Decane	0.090	617.59	0.4842	0.5	48.94	4.40		
98.01	1,2,3-Trimethylbenzene	1.187	664.53	0.3664	0.4	48.58	57.67		
98.13	1-Methyl-3-i-propylbenzene	0.154	667.00	0.2743	0.4	44.55	6.88		
99.04	Indan	0.364	684.90	0.3098	0.4	47.82	17.42		
100.58	1,3-Diethylbenzene	0.208	663.00	0.3497	0.4	47.66	9.89		
100.82	1-Methyl-3-n-propylbenzene	0.571	654.57	0.4098	0.5	49.58	28.29		
101.16	1,4-Diethylbenzene	0.299	657.96	0.4035	0.5	49.63	14.83		
101.25	n-Butylbenzene	0.162	660.55	0.3917	0.5	49.35	7.99		
101.41	1,3-Dimethyl-5-ethylbenzene	0.470	665.36	0.4140	0.4	50.86	23.90		
102.19	1-Methyl-2-n-propylbenzene	0.224	662.40	0.4051	0.5	50.15	11.24		
103.06	1,4,Dimethyl-2-ethylbenzene	0.313	670.68	0.4013	0.4	50.80	15.89		
103.22	1,3-Dimethyl-4-ethylbenzene	0.271	664.41	0.4147	0.4	50.79	13.79		
103.73	1,2-Dimethyl-4-ethylbenzene	0.494	666.25	0.4141	0.4	50.95	25.18		
105.44	1,2-Dimethyl-3-ethylbenzene	0.117	680.00	0.3621	0.4	49.86	5.83		
106.42	1,2,4,5-Tetramethylbenzene	0.246	675.15	0.4350	0.4	52.83	12.98		
106.69	1,2,3,5-Tetramethylbenzene	0.332	681.45	0.3943	0.4	51.54	17.10		
107.97	5-Methylindan	0.073	709.60	0.3524	0.4	52.20	3.81		
108.70	4-Methylindan	0.079	720.90	0.3533	0.4	53.31	4.22		
108.99	2-Methylindan(1)	0.109	693.33	0.3435	0.4	50.23	5.49		
110.69	1-t-Butyl-3,5-dimethylbenzene	0.097	684.00	0.3590	0.4	50.09	4.85		

FACE H:

TIME	COMPONENT	%MOL	Tc, (K)	Accentric Factor	Tr	HOV (kJ/kg)	HOVi (kJ/kg)	MW gasoline (g/mol)	HOV total KJ/Kg
8.77	i-Butane	0.075	407.85	0.1770	0.7	18.69	1.40	97.5	366.84
9.92	n-Butane	4.618	425.16	0.1931	0.7	20.63	95.24		
14.73	i-Pentane	2.874	460.43	0.2275	0.6	24.66	70.87		
16.35	Pentene-1	0.252	464.7778	0.233	0.6	25.20	6.34		
17.16	2-Methylbutene-1	0.539	465.3722	0.2287	0.6	25.14296	13.55		
17.66	n-Pentane	0.724	469.7056	0.2486	0.6	26.07192	18.87		
18.74	t-Pentene-2	0.680	475.9278	0.2406	0.6	26.42275	17.98		
19.73	c-Pentene-2	0.377	475.3722	0.2373	0.6	26.28118	9.91		
20.37	2-Methylbutene-2	1.099	470.9278	0.2767	0.6	26.94716	29.62		
22.39	2,2-Dimethylbutane	2.746	488.7778	0.2339	0.6	27.39035	75.22		
24.92	Cyclopentene	0.155	507	0.1946	0.6	27.79644	4.32		
26.14	3-Methylpentene-1	0.052	494.8389	0.2652	0.6	28.8561	1.51		
26.66	Cyclopentane	8.614	511.7611	0.1943	0.6	28.18762	242.81		
27.37	2,3-Dimethylbutane	0.323	499.9778	0.2476	0.6	28.79864	9.30		
27.78	2,3-Dimethylbutene-1	0.054	500	0.227	0.6	28.18059	1.52		
28.37	2-Methylpentane	1.258	497.5	0.2781	0.6	29.48588	37.10		
28.82	4-Methyl-t-pentene-2	0.095	514	0.2445	0.6	29.95702	2.85		
30.86	3-Methylpentane	0.816	504.4278	0.2773	0.6	30.1056	24.58		
32.00	2-Methylpentene-1	0.167	507	0.2406	0.6	29.21338	4.88		
32.21	Hexene-1	0.095	503.75	0.28	0.6	30.12505	2.86		
34.26	c-Hexene-3	0.053	507.7222	0.2906	0.6	30.82132	1.62		
34.38	n-Hexane	0.508	507.3722	0.3047	0.6	31.22332	15.87		
35.00	t-Hexene-3	0.153	508.55	0.2879	0.6	30.81539	4.72		
35.44	t-Hexene-2	0.232	513	0.2613	0.6	30.39569	7.04		
35.90	2-Methylpentene-2	0.261	514	0.2445	0.6	29.95702	7.81		
36.29	3-Methyl-c-pentene-2	0.169	515.2889	0.2585	0.6	30.5144	5.16		
37.16	c-Hexene-2	0.127	513	0.2722	0.6	30.73799	3.92		
38.40	3-Methyl-t-pentene-2	0.260	519.4278	0.2563	0.6	30.81691	8.02		
38.88	Methylcyclopentane	1.067	532.7889	0.2302	0.6	31.1416	33.24		
40.37	2,4-Dimethylpentane	0.620	519.7889	0.3018	0.6	32.30902	20.05		
43.53	Benzene	1.390	562.1611	0.2108	0.5	32.96582	45.81		
43.71	1-Methylcyclopentene	0.297	541.99	0.219	0.6	31.55289	9.37		
45.01	2-Methyl-c-hexene-3	0.175	528.9611	0.3123	0.6	33.51843	5.87		
45.27	Cyclohexane	0.146	553.5389	0.2149	0.5	32.38858	4.72		
47.87	4,4-Dimethyl-c-pentene-2	0.064	527.0722	0.2755	0.6	32.13185	2.05		
48.21	2-Methylhexane	2.912	530.3722	0.3282	0.6	34.17911	99.54		
49.91	3-Methylhexane	2.347	535.25	0.3216	0.6	34.42701	80.79		
50.67	1,5-Heptadiene	0.341	545	0.2949	0.5	34.43331	11.73		

51.21	1c,3-Dimethylcyclopentane	0.269	550.9278	0.2737	0.5	34.23558	9.22
51.78	1t,2-Dimethylcyclopentane	0.220	553.15	0.2698	0.5	34.29795	7.53
51.94	3-Ethylpentane	0.226	540.6389	0.3094	0.6	34.52465	7.81
52.33	2,2,4-Trimethylpentane	0.493	543.9611	0.3031	0.5	34.61988	17.07
54.39	1,3-Pentadiene, 2,3-dimethyl-	0.074	493.39	0.251	0.6	28.30472	2.10
54.70	C7 - MonoNaph - 1	0.059	604.26	0.243	0.5	37.76193	2.21
54.78	t-Heptene-3	0.077	539.7278	0.3379	0.6	35.40951	2.72
55.16	n-Heptane	12.862	540.2056	0.3494	0.6	35.84802	461.06
55.32	3-Methyl-c-hexene-2	0.072	547.4722	0.3096	0.5	35.17371	2.53
55.57	2-Methyl-2-hexene	0.087	542.8222	0.3128	0.5	34.84685	3.03
55.79	3-Methyl-t-hexene-3	0.066	541.9722	0.3065	0.6	34.55068	2.27
56.14	t-Heptene-2	0.067	549	0.2942	0.5	34.77852	2.32
56.52	Cyclopentene, 1,5-dimethyl-	0.059	573.63	0.245	0.5	35.20151	2.06
56.96	3-Methyl-t-hexene-2	0.071	546.42	0.307	0.5	34.98468	2.48
57.68	2,3-Dimethylpentene-2	0.065	528.4778	0.2852	0.6	32.57976	2.13
58.17	1c,2-Dimethylcyclopentane	0.577	565.15	0.2662	0.5	35.24059	20.33
59.09	1,1,3-Trimethylcyclopentane	0.049	571.3	0.252	0.5	35.25961	1.72
60.77	Ethylcyclopentane	0.179	569.5222	0.2715	0.5	35.82524	6.42
61.64	2,5-Dimethylhexane	0.230	550	0.3576	0.5	37.09404	8.53
61.94	2,4-Dimethylhexane	0.334	553.5	0.3436	0.5	36.94266	12.32
62.69	1c,2t,4-Trimethylcyclopentane	0.090	582.21	0.265	0.5	36.70804	3.29
63.10	3,3-Dimethylhexane	0.062	562	0.32	0.5	36.91004	2.31
64.78	2,3,4-Trimethylpentane	0.159	566.3	0.3161	0.5	37.17234	5.91
65.01	1-Ethylcyclopentene	0.093	578.4	0.27	0.5	36.56047	3.40
65.37	Toluene	11.932	591.7889	0.2641	0.5	37.51774	447.66
67.14	2,3-Dimethylhexane	0.227	563.4	0.3472	0.5	38.03158	8.65
68.41	2-Methylheptane	0.750	559.6389	0.3769	0.5	38.7363	29.05
68.65	4-Methylheptane	0.427	561.7389	0.3711	0.5	38.7361	16.55
69.46	1,3-dimethyl-t-cyclohexane	0.092	596.15	0.2379	0.5	36.86477	3.38
69.69	3-Methylheptane	0.907	563.6722	0.3716	0.5	38.94627	35.32
69.84	3-Ethylhexane	0.204	565.4	0.3628	0.5	38.79594	7.90
71.46	2,2,5-Trimethylhexane	0.131	568.05	0.3567	0.5	38.83186	5.07
71.80	3c-Ethylmethylcyclopentane	0.089	585.2	0.252	0.5	36.47154	3.26
72.00	2t-Ethylmethylcyclopentane	0.053	585.2	0.252	0.5	36.47154	1.93
73.58	5-Methyl-3-heptene	0.056	568.55	0.3839	0.5	39.88389	2.25
73.83	1c,4-Dimethylcyclohexane	0.118	598.15	0.2311	0.5	36.7651	4.33
74.07	n-Octane	0.633	568.8278	0.3962	0.5	40.36574	25.55
76.44	Cyclopentane, 1-ethyl-2-methyl	0.056	585.2	0.252	0.5	36.47154	2.04
77.53	2,4-Dimethylheptane	0.073	576.8	0.39	0.5	40.94034	2.99
78.01	Ethylcyclohexane	0.097	609.15	0.2455	0.5	38.28254	3.70
78.44	2,6-Dimethylheptane	0.072	576.6	0.3955	0.5	41.12737	2.98
79.30	2,5-Dimethylheptane	0.176	581.1	0.393	0.5	41.48712	7.29
79.45	C9 - MonoNaph - 2	0.055	612.06	0.267	0.5	39.4156	2.15

80.47	Ethylbenzene	3.143	617.1722	0.3036	0.5	41.38615	130.09
80.79	1c,2t,4t-Trimethylcyclohexane	0.050	621.87	0.28	0.5	40.82224	2.05
81.62	m-Xylene	4.906	617.05	0.326	0.5	42.30627	207.56
81.75	p-Xylene	2.090	616.2611	0.3259	0.5	42.22847	88.27
81.93	2,3-Dimethylheptane	0.073	589.6	0.385	0.5	42.03132	3.08
82.56	4-Ethylheptane	0.056	584.95	0.416	0.5	42.75989	2.40
82.94	4-Methyloctane	0.205	587.65	0.413	0.5	42.9214	8.79
83.06	2-Methyloctane	0.258	586.75	0.4217	0.5	43.16538	11.15
83.69	Heptane, 3-ethyl-	0.064	594.3	0.3798	0.5	42.29507	2.73
83.85	3-Methyloctane	0.292	590.15	0.4125	0.5	43.15814	12.61
84.35	o-Xylene	2.548	630.3722	0.3127	0.5	42.97798	109.51
85.26	Cyclohexane, 1-ethyl-4-methyl-, trans-	0.052	612.06	0.267	0.5	39.4156	2.05
87.09	n-Nonane	0.214	594.6389	0.4368	0.5	44.57527	9.52
88.21	i-Propylbenzene	0.167	631.15	0.3377	0.5	44.12254	7.36
89.97	Propylcyclohexane	0.070	639.15	0.2595	0.5	41.45843	2.92
90.90	2,6-Dimethyloctane	0.053	606.56	0.426	0.5	45.38224	2.39
91.38	n-Propylbenzene	0.633	638.3778	0.3462	0.5	45.17335	28.58
92.18	1-Methyl-3-ethylbenzene	1.772	637.15	0.3221	0.5	44.00853	78.00
92.38	1-Methyl-4-ethylbenzene	0.785	640.15	0.3242	0.5	44.37804	34.82
92.97	1,3,5-Trimethylbenzene	0.801	637.3611	0.3985	0.5	47.35311	37.94
93.68	4-Methylnonane	0.072	619	0.4	0.5	45.57862	3.28
93.92	1-Methyl-2-ethylbenzene	0.674	637.3611	0.3985	0.5	47.35311	31.89
94.57	3-Methylnonane	0.119	613.7	0.4565	0.5	47.37684	5.63
95.42	1,2,4-Trimethylbenzene	2.352	649.1278	0.3792	0.5	47.66494	112.09
96.91	i-Butylbenzene	0.060	650.15	0.3811	0.5	47.84989	2.89
97.17	sec-Butylbenzene	0.063	664.5389	0.2756	0.4	44.39208	2.82
97.26	n-Decane	0.075	617.5944	0.4842	0.5	48.94242	3.67
98.00	1,2,3-Trimethylbenzene	0.462	664.5278	0.3664	0.4	48.57816	22.44
98.13	1-Methyl-3-i-propylbenzene	0.072	667	0.2743	0.4	44.54745	3.20
99.03	Indan	0.261	684.9	0.3098	0.4	47.8165	12.47
99.33	Indene	0.087	687	0.3352	0.4	49.23215	4.27
100.58	1,3-Diethylbenzene	0.180	656.9	0.3969	0.5	49.22761	8.85
100.81	1-Methyl-3-n-propylbenzene	0.371	654.5722	0.4098	0.5	49.57901	18.38
101.15	1,4-Diethylbenzene	0.220	657.9611	0.4035	0.5	49.6332	10.92
101.25	n-Butylbenzene	0.128	660.55	0.3917	0.5	49.35216	6.34
101.40	1,3-Dimethyl-5-ethylbenzene	0.317	665.3611	0.414	0.4	50.85713	16.11
102.18	1-Methyl-2-n-propylbenzene	0.120	662.4	0.4051	0.5	50.15001	6.01
103.05	1,4,Dimethyl-2-ethylbenzene	0.238	670.6833	0.4013	0.4	50.80021	12.09
103.21	1,3-Dimethyl-4-ethylbenzene	0.218	664.4111	0.4147	0.4	50.79365	11.07
103.72	1,2-Dimethyl-4-ethylbenzene	0.394	666.25	0.4141	0.4	50.95134	20.09
105.44	1,2-Dimethyl-3-ethylbenzene	0.097	680	0.3621	0.4	49.86109	4.85
106.42	1,2,4,5-Tetramethylbenzene	0.161	675.15	0.435	0.4	52.83244	8.52
106.68	1,2,3,5-Tetramethylbenzene	0.221	681.45	0.3943	0.4	51.53632	11.40

107.96	5-Methylindan	0.161	709.6	0.3524	0.4	52.19604	8.40
108.48	1,3-Di-i-propylbenzene	0.061	684	0.359	0.4	50.09473	3.07
108.69	4-Methylindan	0.180	720.9	0.3533	0.4	53.30686	9.59
109.00	2-Methylindan(1)	0.136	693.33	0.3435	0.4	50.2257	6.84
110.49	C12 - IsoParaffin - 5	0.060	666	0.4909	0.4	54.47837	3.27
110.69	1-t-Butyl-3,5-dimethylbenzene	0.282	684	0.359	0.4	50.09473	14.12
111.28	Dimethyl Indane - 1	0.050	722.13	0.252	0.4	48.1989	2.40
114.88	Diimethyl Indene - 2	0.064	722.13	0.252	0.4	48.1989	3.07
116.98	2-Methylnaphthalene	0.230	761	0.3731	0.4	58.16958	13.41
117.75	n-Tridecane	0.095	676.1	0.6186	0.4	61.59819	5.86

Thermograms for all sample runs:

Isooctane Run 1:

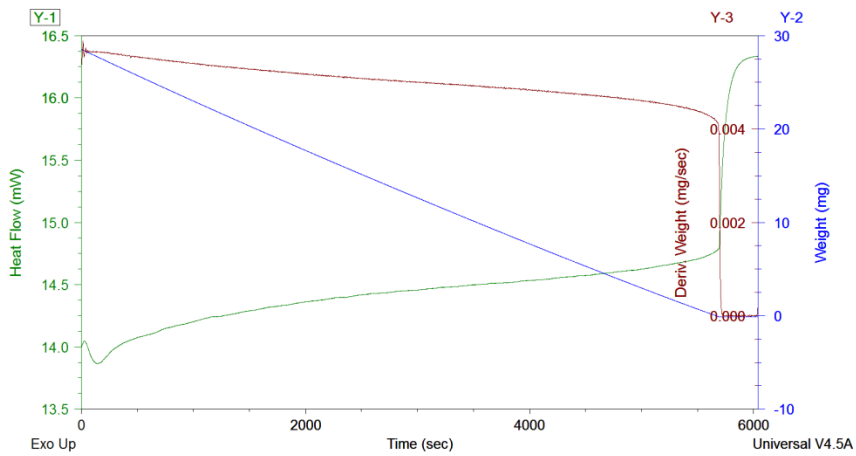

Isooctane Run 2:

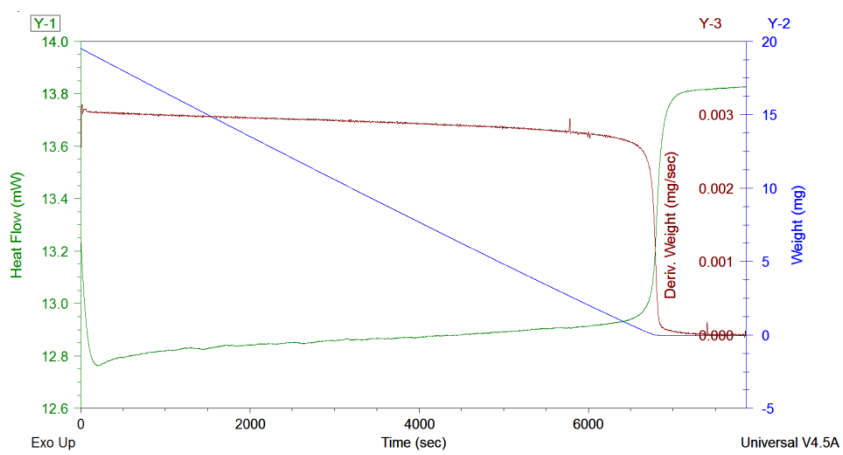

FACE A Run 1:

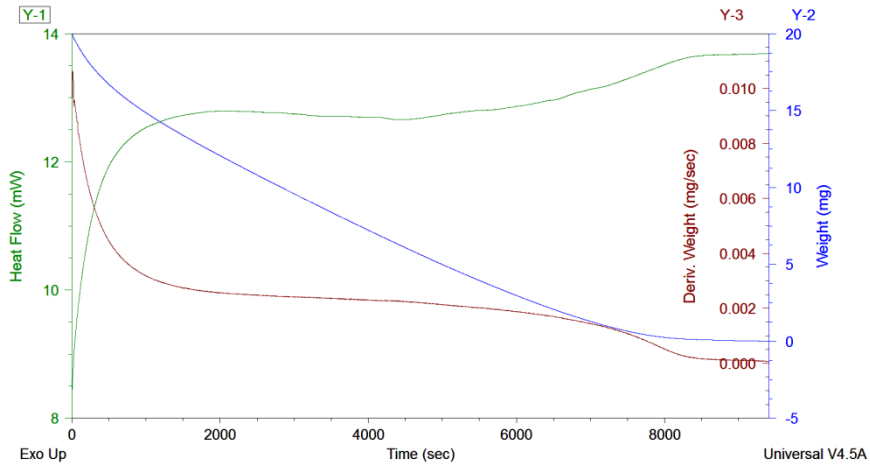

FACE A Run 2:

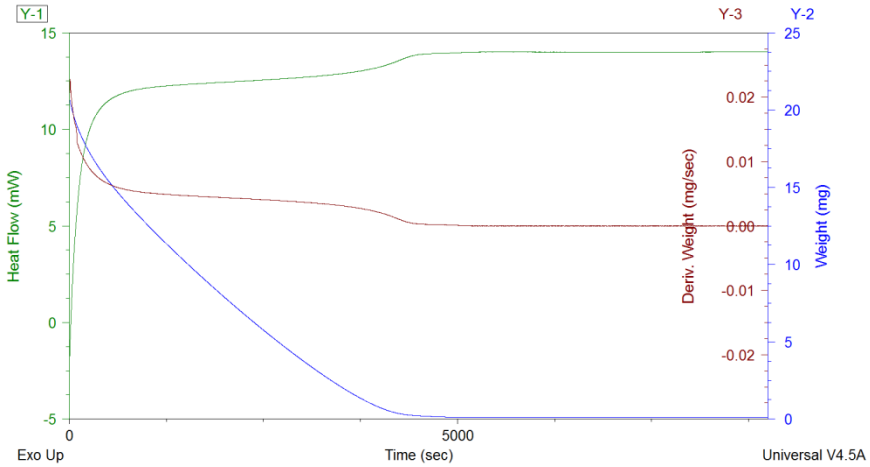

FACE A E10 Run 1:

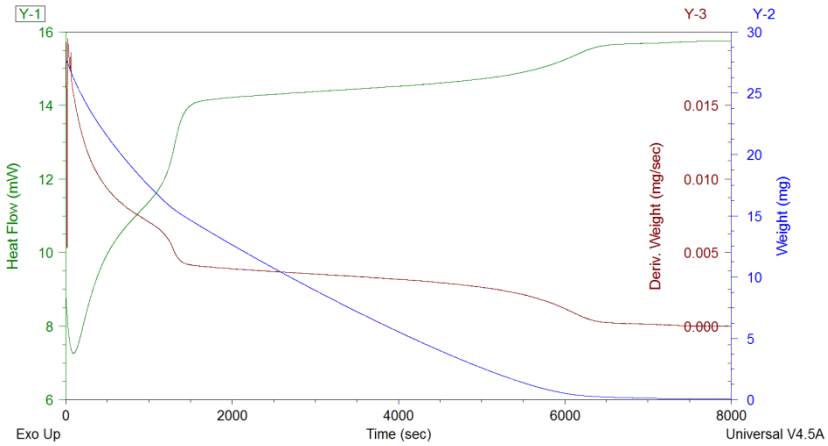

FACE A E10 Run 2:

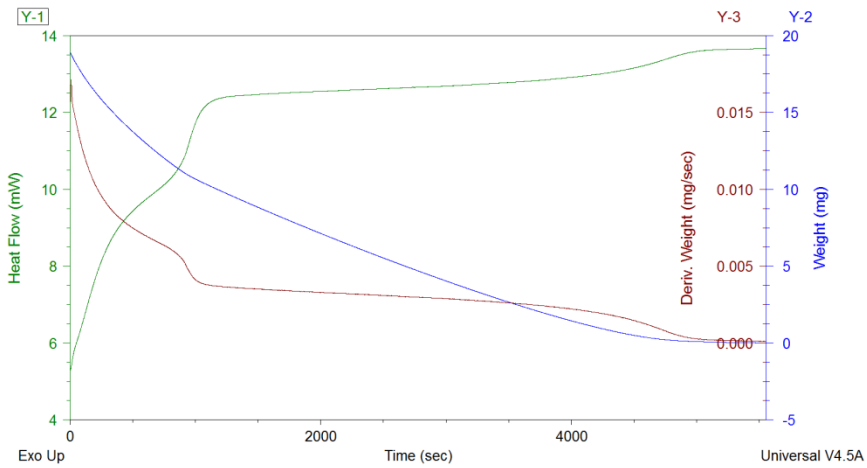

FACE A E15 Run 1:

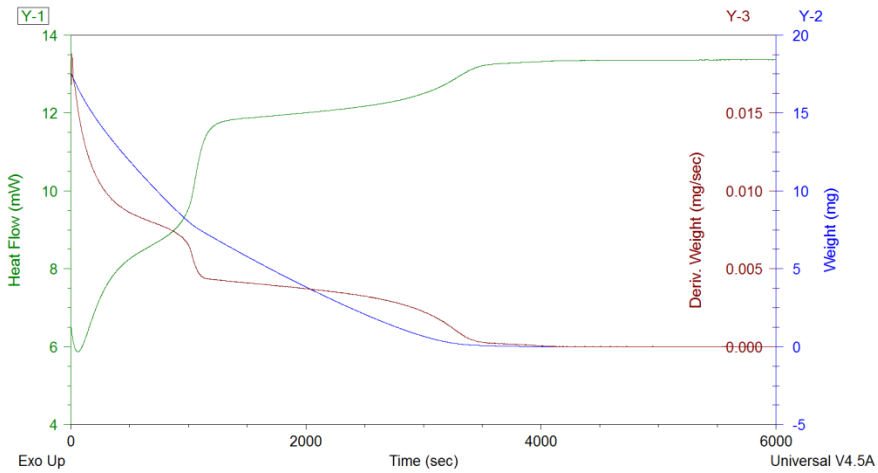

FACE A E15 Run 2:

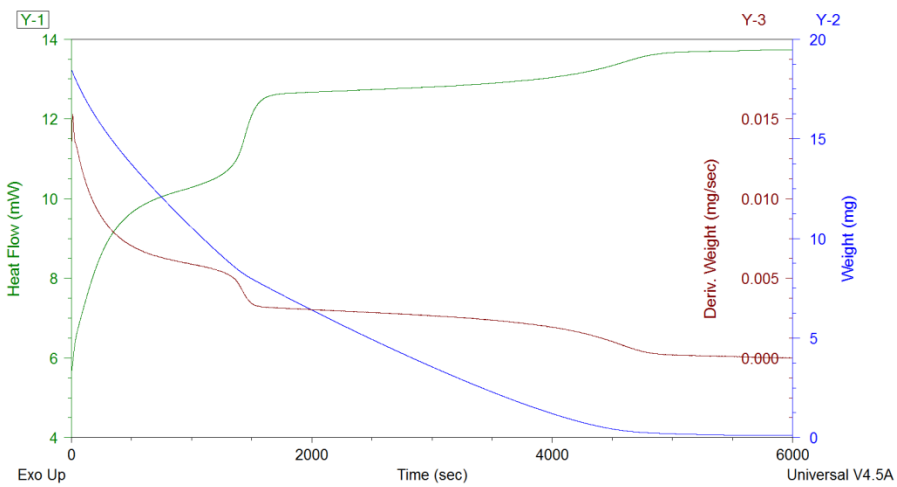

FACE A E30 Run 1:

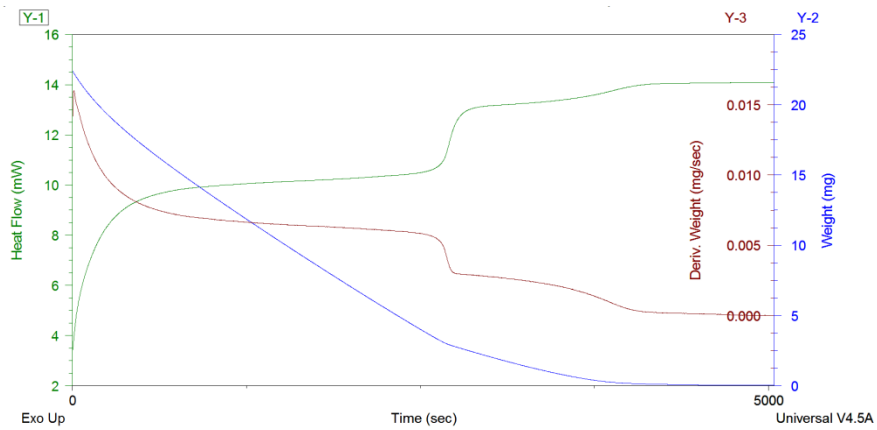

FACE A E30 Run 2:

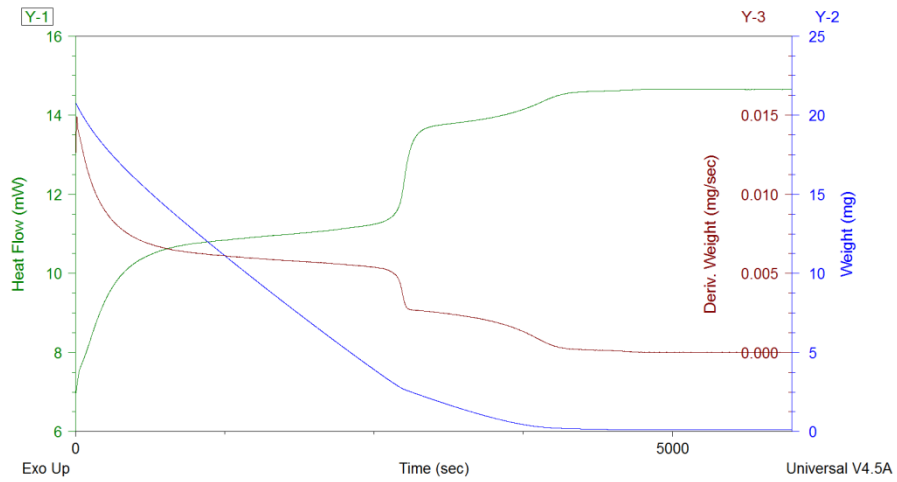

FACE D Run 1:

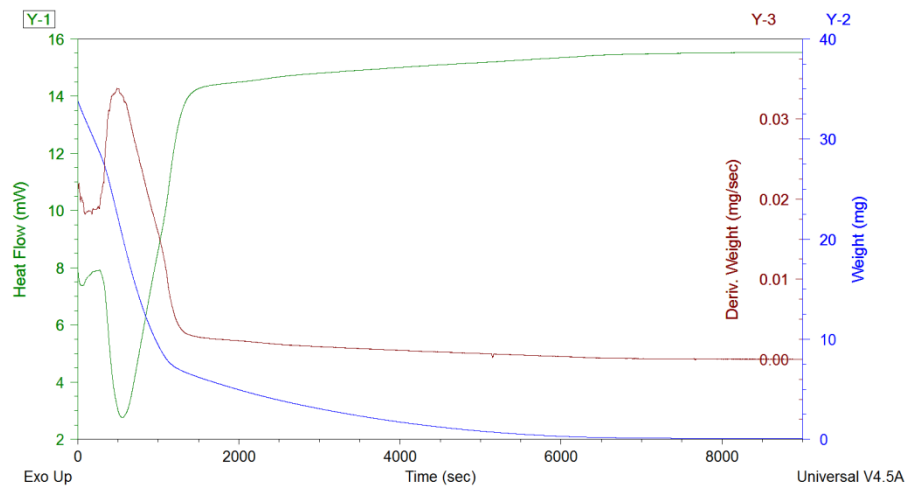

FACE D Run 2:

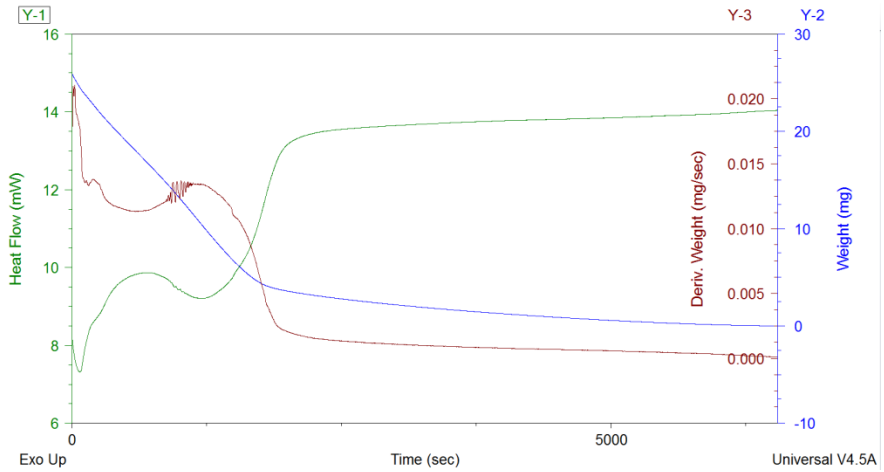

FACE H Run 1:

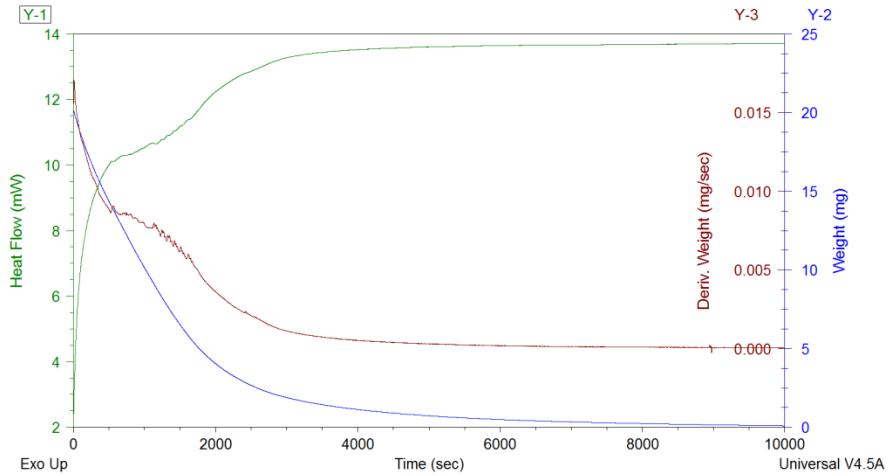

FACE H Run 2:

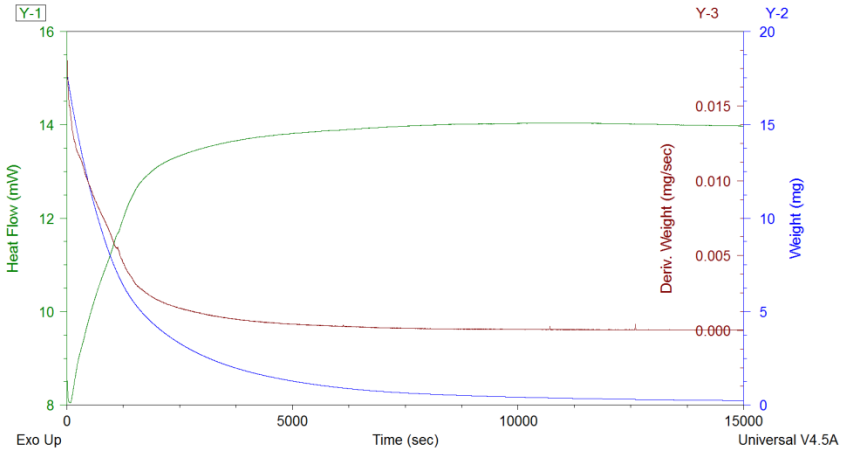

FACE H E10 Run 1:

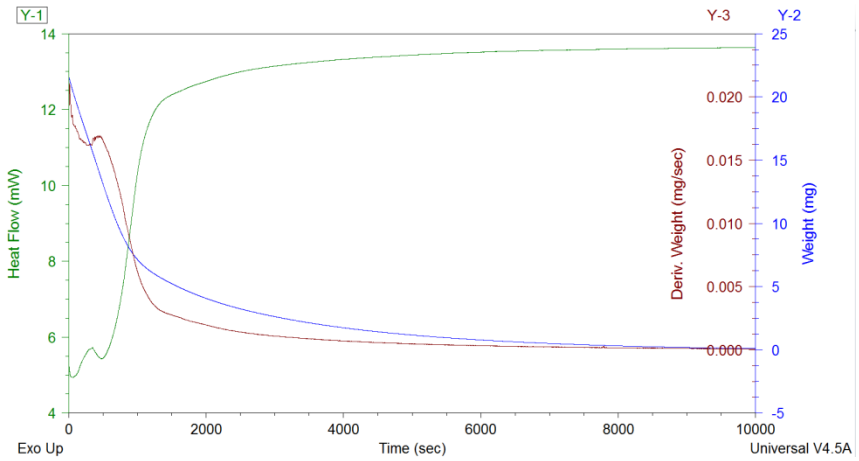

FACE H E10 Run 2:

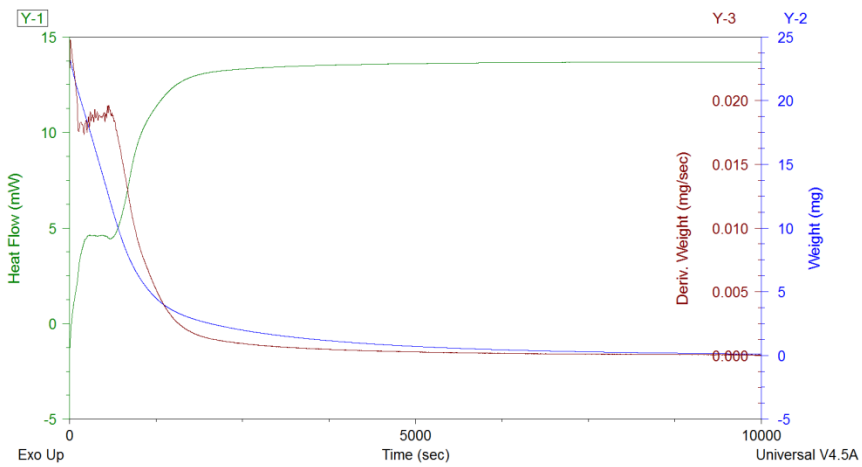

FACE H E15 Run 1:

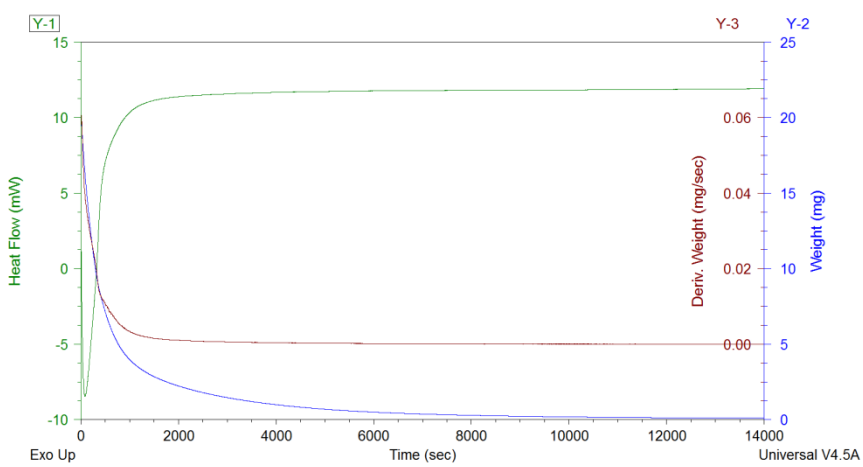

FACE H E15 Run 2:

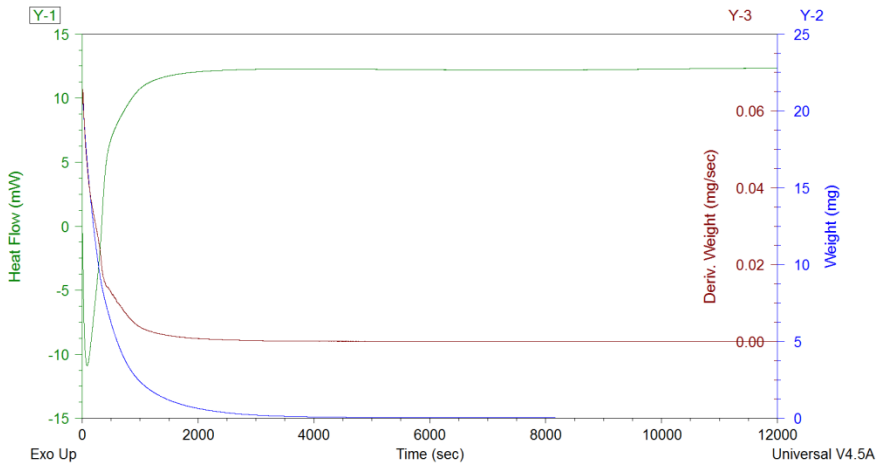

FACE H E30 Run 1:

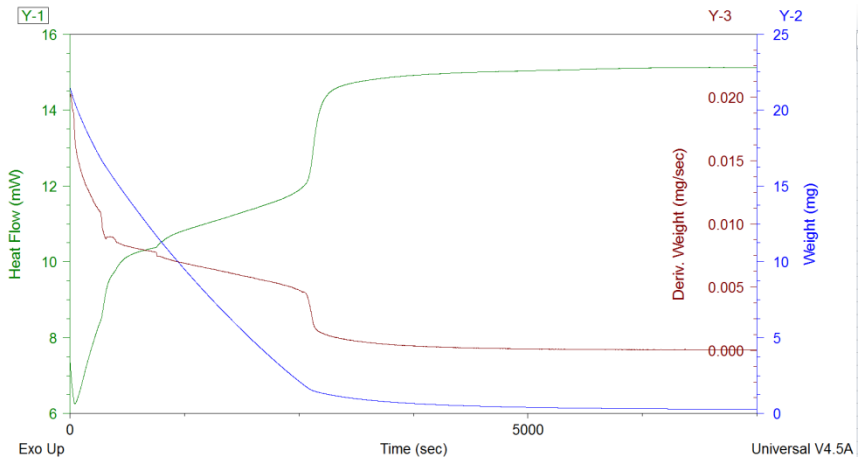

FACE H E30 Run 2:

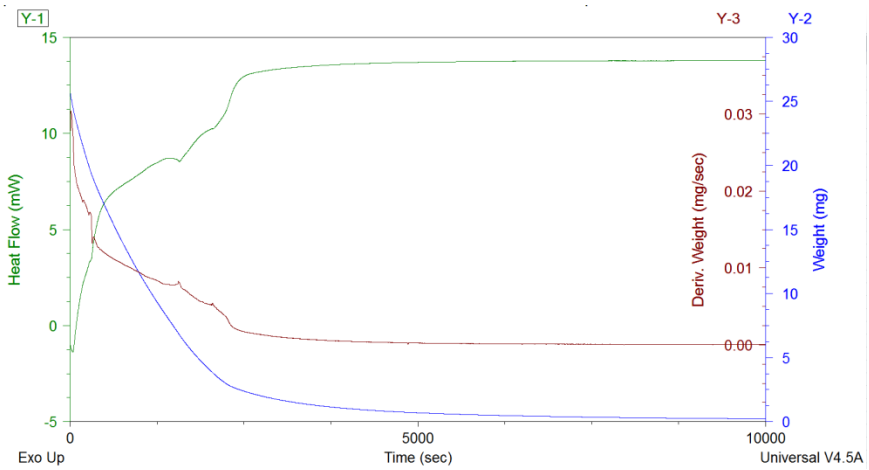

Heat of Vaporization Measurements of Ethanol/Gasoline Blends

Part B

Prepared for
Coordinating Research Council, Inc.
5755 North Point Parkway, Ste. 265
Alpharetta, GA 30022

Prepared by
Steve Sauerbrunn
Scientist
University of Delaware
Center for Composite Materials
Newark, Delaware

CRC Project No. AVFL-27, Phase 1

July 2016

This page intentionally left blank
for back-to-back printing

Executive Summary

This is the final and closing report for project CRC-AVFL-27 "Heat of Vaporization Measurements of Ethanol/Gasoline Blends". The simultaneous thermogravimetric-differential scanning calorimeter (TGA-DSC) was very well suited to the measurement of heat of vaporization (HOV) of these fuels. The measured average HOV values are given in the table below.

Summary of HOV Results

Material	Average HOV	Standard Deviation
	(J/g)	1 σ
FACE Gasoline A	346	8
FACE A & 10% Ethanol	402	na
FACE A & 15% Ethanol	439	na
FACE A & 30% Ethanol	540	na
FACE Gasoline D	364	4
FACE Gasoline H	383	25
FACE H & 10% Ethanol	408	na
FACE H & 15% Ethanol	434	na
FACE H & 30% Ethanol	603	42

"na" indicates that the standard deviation was not available

Table of Contents

page

1. List of Acronyms and Abbreviations ……..……..10
2. Background ……..10
3. Scope …….…….. 12
4. Experimental
4.1. Materials …….……..... 13
4.2. Instrumental …….… 13
4.3 Temperature calibration …….…….….. 13
4.4 Sample Preparation for Testing……..……..….. 13
4.5 Liquid Density Measurement……..15
4.6 Coolant Temperature Adjustment……...15
4.7 HOV Literature Values for Pure Liquids……....16
4.8 Testing Method……...16
4.9 Data Evaluation Procedure……..17
4.10 Heat Flow Calibration…….…….….20
4.11 HOV Validation with Ethanol……...……20
4.12 HOV Validation with Iso-Octane……..21
4.13 Gasoline/Ethanol Mixture Preparation……..22

5. Results
5.1 HOV of Toluene…….…….23
5.2 HOV of Isooctane……..……..….23
5.3 HOV of n-Octane……..23
5.4 HOV of FACE Gasoline A…….….24
5.5 HOV of FACE Gasoline D……..24
5.6 HOV of FACE Gasoline H……..……24
5.7 HOV of FACE A with 10%Ethanol……..……..25
5.8 HOV of FACE A with 15% Ethanol…….…….…….25
5.9 HOV of FACE A with 30% Ethanol……..…….25
5.10 HOV of FACE H with 10% Ethanol…….……25
5.11 HOV of FACE H with 15% Ethanol…….26
5.12 HOV of FACE H + 30% Ethanol……...26
5.13 Summary of HOV results……...……27
6. Conclusions……..……..29
7. References……..30
Appendix A ……..……31

List of Figures

Figure 1: TGA/DSC two thermocouple DSC sensor ……....12
Figure 2: An aluminum crucible and two aluminum screens ……...…14
Figure 3: An aluminum crucible with the aluminum screen distribution media……..…..14
Figure 4: An aluminum crucible with the 8 mm aluminum screen crimped……..…...15
Figure 5: Raw TGA/DSC data …….....17
Figure 6: Baseline of zero heat flow ……17
Figure 7: Heat flow baseline subtraction ……. 18
Figure 8: TGA/DSC analysis region ……... 18
Figure 9: TGA/DSC Analysis …….. 19
Figure 10: TGA/DSC increasing precision …….. 19
Figure 11: Validation of the heatflow calibration using the HOV of water …….… 20
Figure 12: Validation using the HOV of Ethanol …… 21
Figure 13: Validation using the HOV of Isooctane …….…….……..….. 21
Figure 14: HOV versus ethanol content in FACE Gasoline A ……..28
Figure 15: HOV versus ethanol content in FACE Gasoline H ……. 28
Figure A1: Evaporation rate versus hole size …….……. 31
Figure A2: Room temperature evaporation rate through crimped ampoules ……..… 33

List of Tables

Table 1: Temperature Calibration …….….... 13
Table 2: Liquid Densities at 23 °C…….15
Table 3: HOV Literature Values for Pure Liquids at 25 °C …….…..... 16
Table 4: Gasoline-Ethanol Mixture Compositions……..……..…….22
Table 5: Testing Conditions …….……. 22
Table 6: HOV of Toluene …….……. 23
Table 7: HOV of Isooctane …….……..…..... 23
Table 8: HOV of n-Octane …….……... 23
Table 9: HOV of FACE Gasoline A ……. 24
Table 10: HOV of FACE Gasoline D …….…….…. 24
Table 11: HOV of FACE Gasoline H …….….. 24
Table 12: HOV of FACE A with 10% Ethanol …….…… 25
Table 13: HOV of FACE A with 15% Ethanol ……. 25
Table 14: HOV of FACE A with 30% Ethanol ……. 25
Table 15: HOV of FACE H with 10% Ethanol ……. 25
Table 16: HOV of FACE H with 15% Ethanol ……. 26
Table 17: HOV of FACE H with 30% Ethanol……...26
Table 18: Summary of HOV Results ……. 27

This page intentionally left blank
for back-to-back printing

1. List of Acronyms and Abbreviations

FACE Gasolines are a matrix of Fuels for Advanced Combustion Engines designed by CRC and manufactured by ChevronPhillips Chemical Co.

DSC is a Differential Scanning Calorimeter instrument.

TGA/DSC is a combination of a Thermogravimetric Analyzer with a Differential Scanning Calorimeter. This instrument measures heat flow as well as sample mass.

HOV or **ΔH_{vap}** is the heat of vaporization. It is the same as the heat of evaporation. This is the heat (energy) associated with the transition from a liquid to a gas. The Heat of Vaporization is also called the Latent Heat of Vaporization or the Molar Enthalpy of Vaporization.

Ethanol in pure, anhydrous, ethanol or 1-hydroxyethane.

J/mol is Joules per mole, the units typically reported for the HOV of a pure substance.

T/C is a thermocouple.

v/v % this is the volume to volume percentage of the gasoline-ethanol mixture.

w/w % is the mass to mass percentage of the gasoline-ethanol mixture.

2. Background

The Coordinating Research Council (CRC) has sponsored this testing for the "**Heat of Vaporization Measurements of Ethanol/Gasoline Blends**" (CRC Project No. AVFL-27). The heat of vaporization (HOV, also symbolized as ΔH_{vap}) is the energy that is needed to completely convert a given quantity of a substance from a liquid to a gaseous state at a given temperature and pressure, usually measured at ambient conditions. For simple substances (neat compounds), the HOV can be calculated from the Clausius-Clapeyron equation [1, 2] by measuring the boiling point of a pure substance at several different pressures, or the vapor pressure at several different temperatures. The approach (e.g., used in ASTM E2071 [3]) gives the HOV for the substance in J/mol.

Heat of vaporization is the amount of heat required to make a physical change from the liquid phase to the gas phase, shown in the equation below.

$$H_2O_{Liquid} \xrightarrow{\Delta H_{Evaporation}} H_2O_{Gas}$$

Heat of vaporization of liquids has been done by several estimation techniques, most notable being the Clausius-Clapeyron equation,

$$\ln\left(\frac{P}{P_0}\right) = -\frac{\Delta H_{Vap}}{RT} + C$$

Where R = gas constant

T = temperature (K)
C = a constant
P = measured pressure
P_0 = reference pressure

The ASTM standard E2071 [3] uses this technique with a high pressure DSC. The technique is limited to liquids that boil within a narrow temperature range, usually pure compounds. Alexander et. al. [4] proposed a technique that uses the TGA to generate evaporation data and uses zero order Arrhenius kinetics and the Clausius-Clapeyron equation to determine the heat of vaporization. Houska et. al. [5] used a technique that measured the relative humidity (%RH) above a hydrated sample at several temperatures and amounts of hydration. The %RH data was converted into partial pressure of water and the Clausius-Clapeyron equation was used to determine the heat of vaporization. All of these tests are an estimation of the heat of vaporization because they all assume an ideal gas behavior, which is the basic assumption of the Clausius-Clapeyron equation.

Engineers that design internal combustion engines need the HOV in units of energy per mass, such as J/g, in order to improve the fuel efficiency of new engine designs. The HOV of multicomponent, volatile blends, such as gasoline and gasoline-ethanol mixtures, must be measured directly and cannot be measured using the Clausius-Clapeyron equation.

For liquid fuels in combustion engines, droplet vaporization and heat transfer have long been recognized as important factors for optimizing vehicle performance and emissions from gasoline engines [6]. Charge cooling of the injected air/fuel mixture occurs when liquid fuel is injected into the engine's intake air system or directly into the cylinder and the fuel droplets begin to vaporize. The vaporization of the liquid droplets extracts energy from the air/fuel mixture and reduces its temperature. A cooler air/fuel mixture is expected to increase the engine's volumetric efficiency and power output and improve knock resistance but too much charge cooling could result in vehicle driveability problems [7]. Knock typically occurs under conditions where the air/fuel charge has fully evaporated. In contrast, driveability issues typically occur when a significant portion of the charge has not evaporated.

To understand the impact of fuel properties on these effects, the HOV is an important parameter because it provides a direct measure of the charge-cooling effectiveness of the fluid when it is vaporized. Generally accepted HOV values for hydrocarbon-only gasoline and for neat ethanol can be found in [7] but there are relatively few references for HOV measurements on low-level blends of ethanol and gasoline [8,9].

The objective of this CRC project is to develop or validate experimental methods to obtain accurate HOV data for multicomponent liquids in order to better understand the variation in charge-cooling of liquid fuels in combustion engines.

The HOV is easily measured with a simultaneous TGA/DSC. The TGA measures the rate of mass loss and the heat flow sensor of the TGA/DSC measures the rate of heat loss during the vaporization process. This technique gives a continuous measurement of the HOV through the entire vaporization process. This will give much more information about the evaporation of liquid fuel blends than the single HOV value for the entire fuel. There might be an azeotropic composition that occurs during vaporization. This technique would allow the measurement of the azeotrope HOV. The HOV measured through the vaporization process can also be integrated to give one single average HOV value for the entire fuel blend.

The simultaneous TGA-DSC test should be widely accepted due to its simple and direct measurement of the heat of vaporization. Heat of vaporization (HOV) is the amount of heat required to make a physical change from the liquid phase to the gas phase. This heat cannot be

measured with a DSC alone because the sample changes weight as the phase transition proceeds. This heat cannot be measured by TGA alone because it does not measure the heat flow into the sample. The TGA/DSC, however, measures both the rate of weight loss and the rate of heat flow during the entire evaporation process.

Instead of an estimated measure of the heat of vaporization, it can be directly measured using a simultaneous TGA/DSC instrument. This combined technique offers a direct measure of the heat of vaporation. This concept is shown in the following equation.

$$\frac{J}{g} = \frac{W \times s}{g} = \frac{mW \times s}{mg} = \frac{mW}{mg/s}$$

Watts (W) times seconds (s) can be substituted for the heat (J). Then convert both the heat flow (W) and the mass (g) into mW and mg, respectively. Then move the seconds (s) from the numerator into the denominator. Now one can see that the heat of vaporization is just the heat flow (mW) divided by the rate of mass loss (mg/s). Both of these signals are produced by the TGA/DSC instrument. Also notice that this technique does not require complete evaporation of the sample, nor does it need to be a pure compound.

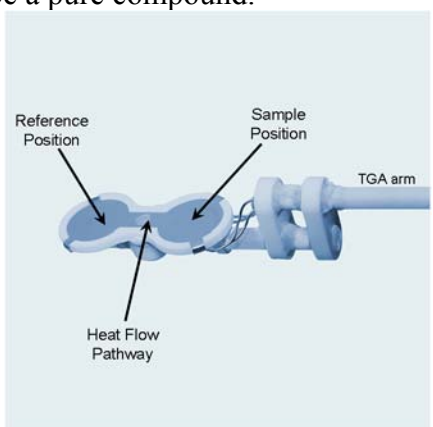

Figure 1: TGA/DSC two thermocouple DSC sensor. The heat flow pathway of this sensor is fixed and can be calibrated to give accurate DSC heat flow response. The surface is made of platinum, for high thermal conductivity, and supported by ceramic holder.

In the current study, the simultaneous TGA/DSC was used to determine the heat of vaporization of multicomponent mixtures. Water is a suitable calibration material and results were confirmed with ethanol. The test is a direct measure of the heat of vaporization. There are no 'ideal gas' approximations required. Additionally, the heat of evaporation can be determined at temperature other than the boiling point of the material. This test should be widely accepted due to its simple direct measurement of heats of vaporization.

3. Scope

The objective of this effort is to provide HOV data on FACE Gasoline A, FACE Gasoline D, FACE Gasoline H and gasoline ethanol blends. The gasoline ethanol blends tested were FACE Gasoline A with 10%, 15% and 30% Ethanol and FACE Gasoline H with 10%, 15% and 30% Ethanol. For reference purposes, HOVs were also measured for several pure components (distilled water, anhydrous ethanol, n-octane, iso-octane, and toluene) to validate the TGA/DSC results against published literature values.

4. Experimental

4.1 Materials

Anhydrous ethanol (100%) was obtained from Decon Laboratories, PN 2716GEA. *n*-Octane (≥99%) was obtained from Aldrich, PN 657042-100ML, lot # 16124AEV. Isooctane (99.8%) was purchased from Sigma-Aldrich, PN 360066-100ML. Toluene (99.8%) was obtained from Sigma-Aldrich, PN 244511-100ML, lot # SHBG3513V. Water was distilled water which was purchased locally. Samples of FACE Gasolines A, D, and H were provided by Bill Cannella (Chevron) [10]. Detailed analyses of the chemical and physical properties of the FACE gasolines are provided in CRC Report No. AVFL-24.

4.2 Instrumental

The Mettler Toledo TGA/DSC1 with a large high temperature furnace was used for this testing. The instrument was equipped with a gas switching box with mass flow controllers. The TGA/DSC was using a DTA sensor. This sensor has two positions, one for the sample pan and one for the empty reference pan. The TGA/DSC was also connected to a refrigerated water recirculating temperature controller (Poly Science Model 9701). The liquids were pipetted with two calibrated Hamilton syringes one 50 µL (PN CAL80900) and one 200 µL (PN CAL81100). The mixtures were prepared in glass vials (Fisherbrand PN 033915) and crimp sealed with PTFE lined red rubber seals (Fisherbrand PN 03-391-3). The seals were covered with aluminum tape to reduce evaporation from the vial through the needle punctures.

4.3 Temperature Calibration

The TGA/DSC was temperature calibrated with an external Omega T type thermocouple that was NIST certified by Omega. The temperature was calibrated isothermally at 50 °C and 200 °C. The calibration was validated with another isothermal test and the results are shown in Table 1.

Table 1: Temperature Calibration

Sample T/C	NIST T/C
50.03 °C	49.8 °C
200.56 °C	200.5 °C

4.4 Sample Preparation for Testing

The liquid sample was pipetted into the aluminum crucible with the 50 µL syringe (see Figures 2-4 for pictures of the crucibles and screens). The 40 µL crucible (Mettler PN ME-26763) was used for liquids that evaporated slowly or had a large HOV, such as water. The larger 100 µL crucible (Mettler PN ME-51119872) was used for liquids that evaporated quickly, such as iso-octane. An aluminum screen 5 mm o.d. was put in the bottom of the crucible. This served as a distribution media so the liquid would not wick into the corners of the crucible. If the liquid wicked into the corners, the evaporation rate would slow at the end of the test and caused the test to be a longer duration. The aluminum screen (200 x 200 mesh) was purchased from McMaster-Carr (PN 9227T67). The same aluminum screen, but with 8 mm o.d., was crimped onto the top of the crucible. The aluminum screen mesh disks were punched from the sheet using 5 and 8

mm hole punches. The 5 mm o.d. disk was cleaned in an oven at 500 °C for one hour in air. This removed organic residue so it would not contaminate the sample.

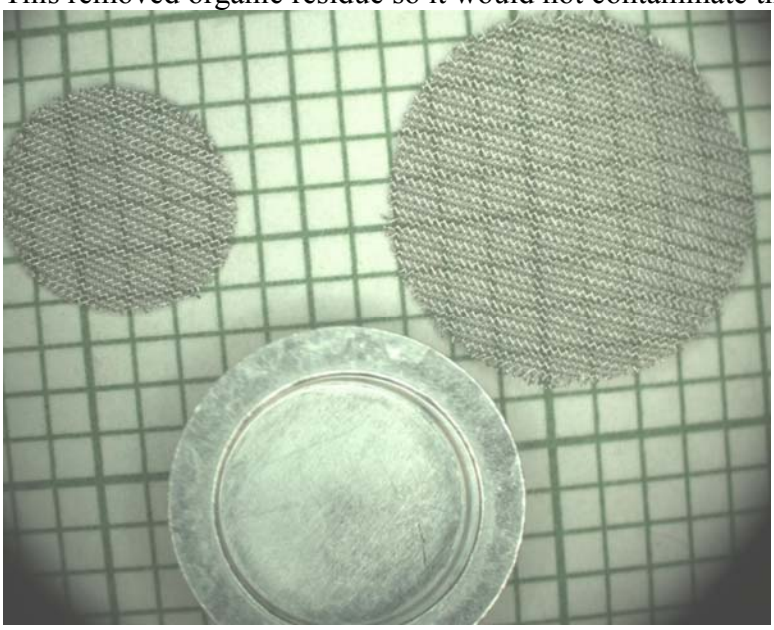

Figure 2: An aluminum crucible and two aluminum screens. The 40 µL crucible, the 5 mm screen and the 8 mm screen are shown here. The background grid in 1mm per square.

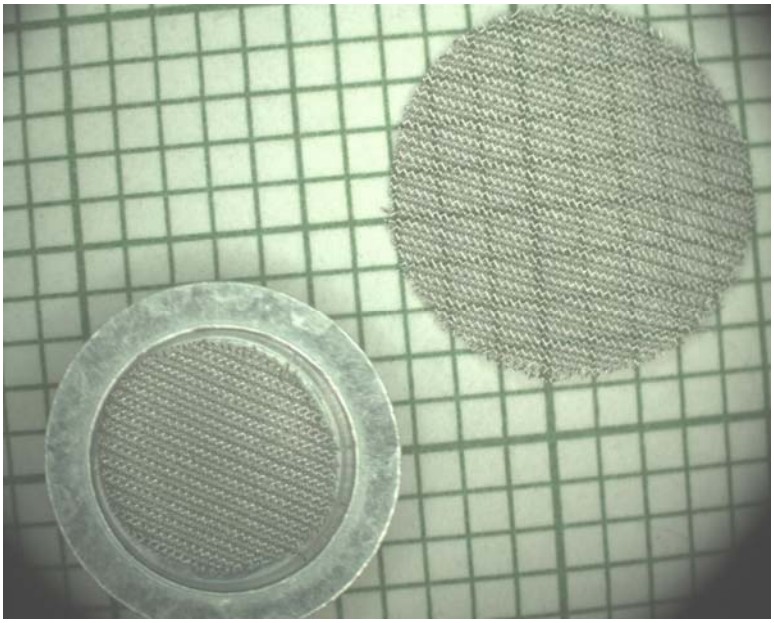

Figure 3: An aluminum crucible with the aluminum screen distribution media.

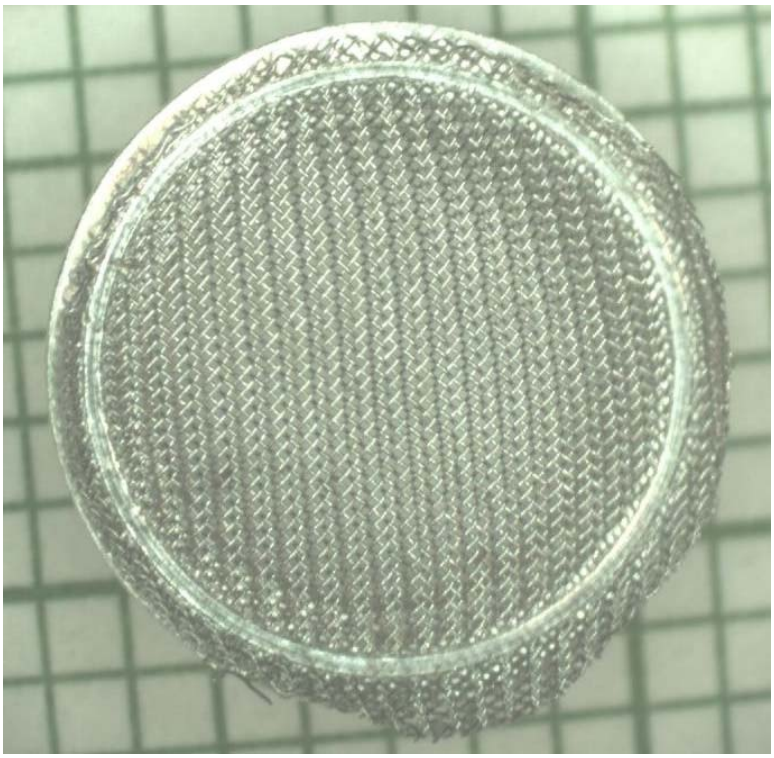
Figure 4: An aluminum crucible with the 8 mm aluminum screen crimped.

4.5 Liquid Density Measurement

The density of liquids was determined gravimetrically using the 200 µL syringe as the volume containing the liquid. The needle of the empty syringe was capped with a piece of rubber. The empty syringe and cap were weighed to get the tare mass. The syringe was filled to the 200 µL mark with the liquid to be measured. The needle was capped with the rubber and weighed. The density was calculated as the mass (g) divided by the volume (0.2 mL). The results are shown in the table below. The syringe volume cannot be read to four significant figures, but these values were used to make up the gasoline-ethanol mixtures.

Table 2: Liquid Densities at 23 °C

Sample	Density (g/mL)
FACE Gasoline A	0.683
Face Gasoline D	0.740
Face Gasoline H	0.762
Ethanol	0.805

4.6 Coolant Temperature Adjustment

The coolant temperature of the refrigerated water recirculating temperature controller was adjusted so that the sample temperature in the TGA/DSC was controlled at 25.0 ± 0.1 °C. This adjustment took several days, but the sample temperature was stable even when the chiller was turned off and back on. The sample temperature was allowed to stabilize overnight after the system had been turned on.

4.7 HOV Literature Values for Pure Liquids

Table 3: HOV Values for Pure Liquids at 25 °C

Sample	HOV[4] at 25 °C (J/g)	HOV at 25 °C [1] (J/g)	Std Devi[2] (J/g)	# of Values Used[2]
Water	2441	2442	4	ΔH_{form}[3]
Ethanol	924	918	9	12
Toluene	412	402	32	9
n-Octane	363	359	35	10
Isooctane	308	307	2	7

1) Literature values were taken from the web site www.webbook.nist.gov . These values represent the average values published in peer reviewed literature.
2) 'N' is the number of values used to calculate the average and standard deviation reported on the www.webbook.nist.gov web site.
3) Calculated from the difference between the delta heat of formation for the gas and liquid water. Heat of formation data was from the web site www.webbook.nist.gov .
4) These data are from the AIChE's DIPPR 801 database and reproduced here with permission. R.L. Rowley , W.V. Wilding , J.L. Oscarson , T.A. Knotts , N.F. Giles , DIPPR data compilation of pure chemical properties, Design Institute for Physical Properties, AIChE, New York, NY, 2016.
AIChE's Design Institute for Physical Properties (DIPPR®) uses reasonable efforts to verify that DIPPR data have been selected on the basis of sound scientific judgment; however, AIChE makes no warranties to that effect and disclaims all warranties, either express or implied, including but not limited to warranties of fitness for a particular purpose.

4.8 Testing Method

The sample was loaded in the crucible and placed in the TGA as quickly as possible. The chilled recirculating water bath was set so that the sample temperature was maintained at 25 ± 0.1 °C without the use of the TGA Furnace. The TGA was setup so that the furnace would never turn on before, during or after the experiment. The experiment was run for 3 hours with a sampling interval of 2 seconds per point. The experiment could be manually stopped prior to the end of the method, if at least 10 minutes of baseline was collected after the test liquid had completely evaporated.

4.9 Data Evaluation Procedure

All analyses were performed using the Mettler Toledo STAR^{e} software. The methods are demonstrated in Figures 5-10.

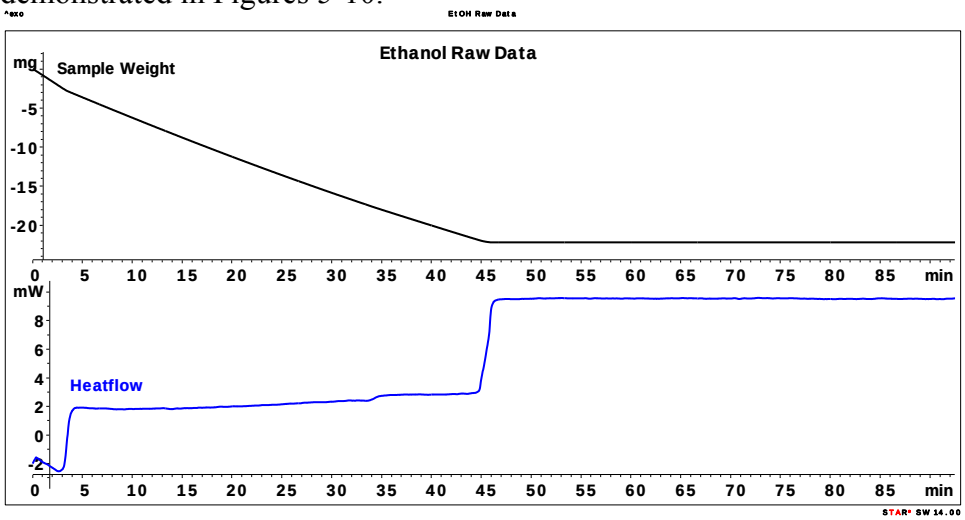

Figure 5: Raw TGA/DSC data. The top black curve is the mass of the sample during evaporation. The bottom blue curve is the heat flow, in mW, as the liquid is evaporating. Endothermic heat flow is shown by negative values (in the down direction).

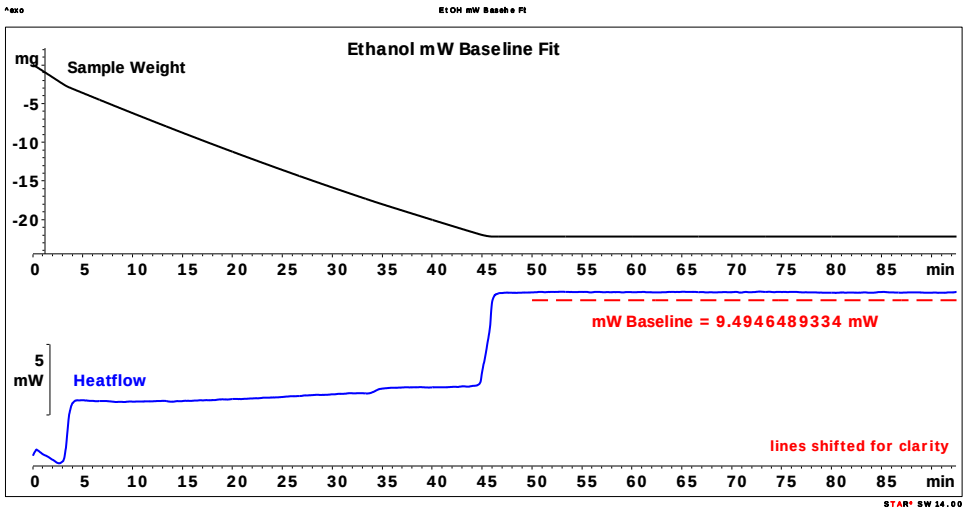

Figure 6: Baseline for zero heat flow (from 50 minutes onward). A polynomial, of zero order, is fit (red line) to the heat flow data from 50 minutes (the end of the evaporation); to the end of the experiment. The dashed curve is shifted vertically so one can see the best fit baseline.

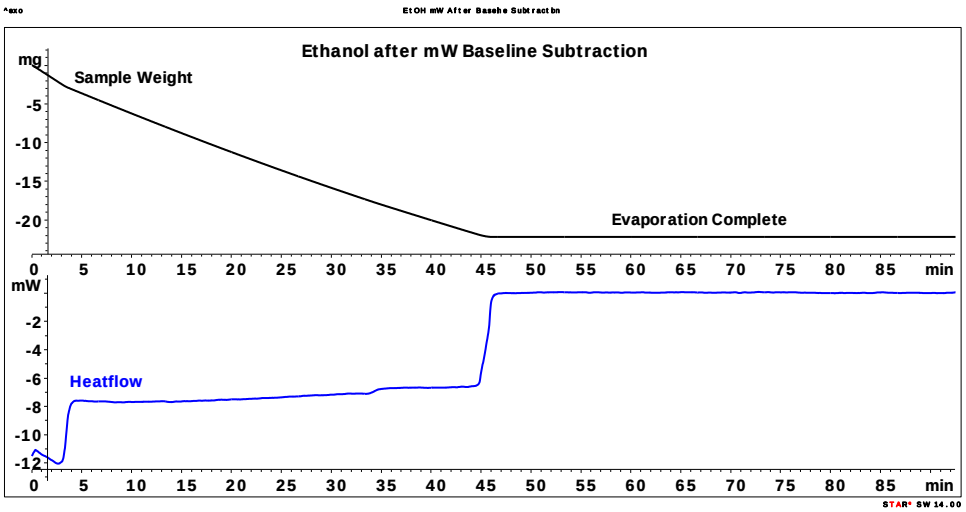

Figure 7: Heat flow baseline subtraction. The mW baseline value from the polynomial fit is subtracted from the heat flow data to give the bottom curve shown.

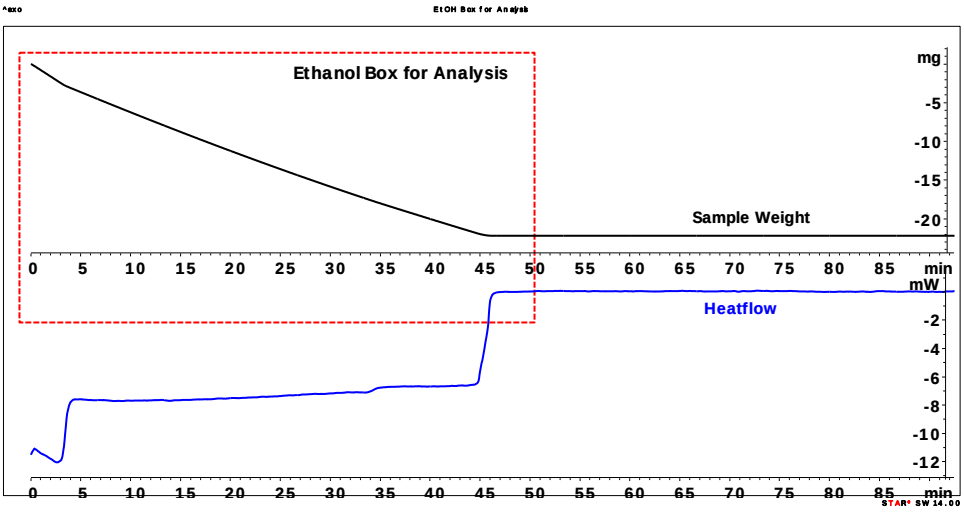

Figure 8: TGA/DSC analysis region. An analysis box is placed over the data from the beginning of the experiment to the point where the sample has completely evaporated, in this case 50 minutes.

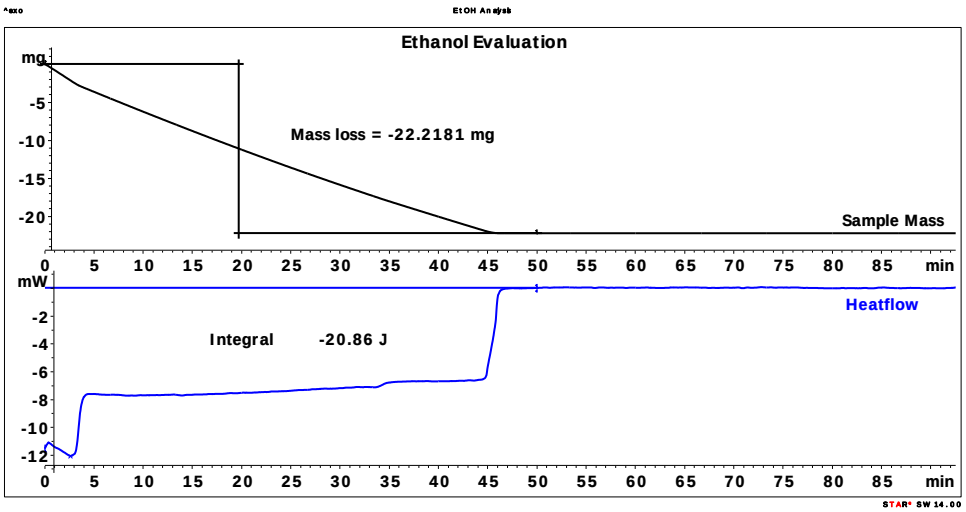

Figure 9: TGA/DSC analysis. The mass loss was calculated using the 'horizontal tangent' option. The enthalpy of evaporation was calculated using the 'zero line' baseline option. In both cases, the analysis was performed from the start of the experiment to the end of the evaporation process, in this case 50 minutes.

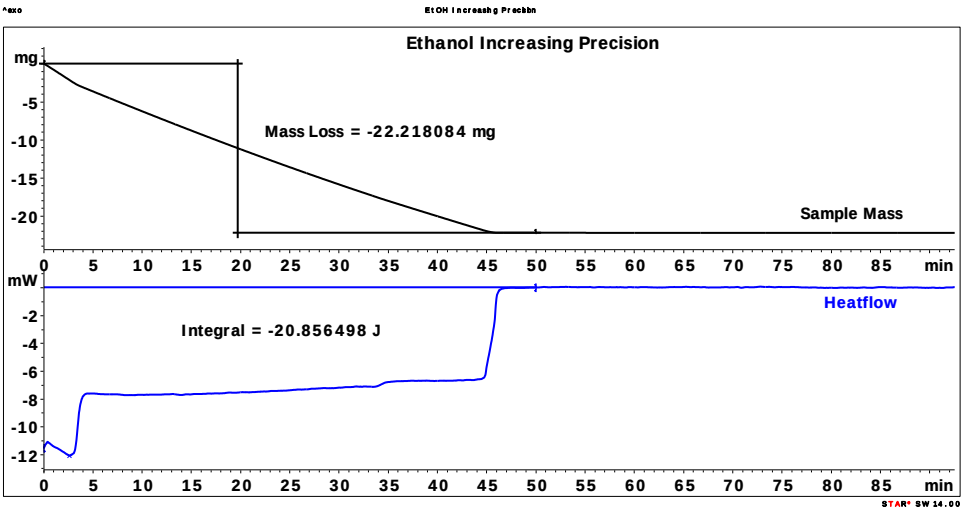

Figure 10: TGA/DSC increasing precision. The mass loss and the integral were increased in precision to 6 values to the right of the decimal. This gives plenty of resolution for the HOV calculation.

4.10 Heat Flow Calibration

Water was used as the heat flow calibrant. The heat of formation for liquid and gas were taken from the NIST Web Book(1).

$$\Delta_{formation} H^0_{liquid} = -285.83\ kJ/mol$$
$$\Delta_{formation} H^0_{gas} = -241.83\ kJ/mol$$

$$HOV = \frac{(285.83 - 241.83)\ {}^{kJ}/_{mol}}{18.0153\ {}^{g}/_{mol}} = \frac{44}{18.0153} = 2.4424\ {}^{kJ}/_{g} = 2{,}443.4\ {}^{J}/_{g}$$

The literature value of 2,443 J/g was used for the HOV of water. The heat flow signal of the TGA-DSC was calibrated using the ratio of the literature HOV to the observed HOV. The TGA-DSC heatflow signal is multiplied by this ratio for all further experiments. After calibration, it is always prudent to double check the calibration with a validation experiment. The results for the validation of the heatflow calibration curves are shown in Figure 11. The top half of the figure is the sample mass and the bottom half is the heatflow, negative is endothermic. The heatflow baseline is the average value after the liquid has completely evaporated, in this case above 117 minutes. The baseline value is subtracted from the sample heatflow. This has already been done in Figure 11. In this example, the heatflow is integrated from the start of the experiment to about 108 minutes, where the baseline starts. The mass loss is taken from the start of the run to the end. The HOV is simply the integrated enthalpy (in Joules) divided by the mass loss (in grams).

Enthalpy 27.985266 J
Mass loss 0.011549662 g
HOV = 2423.038 J/g Lit = 2443 J/g
The measured result is 0.8% low. This is acceptable.

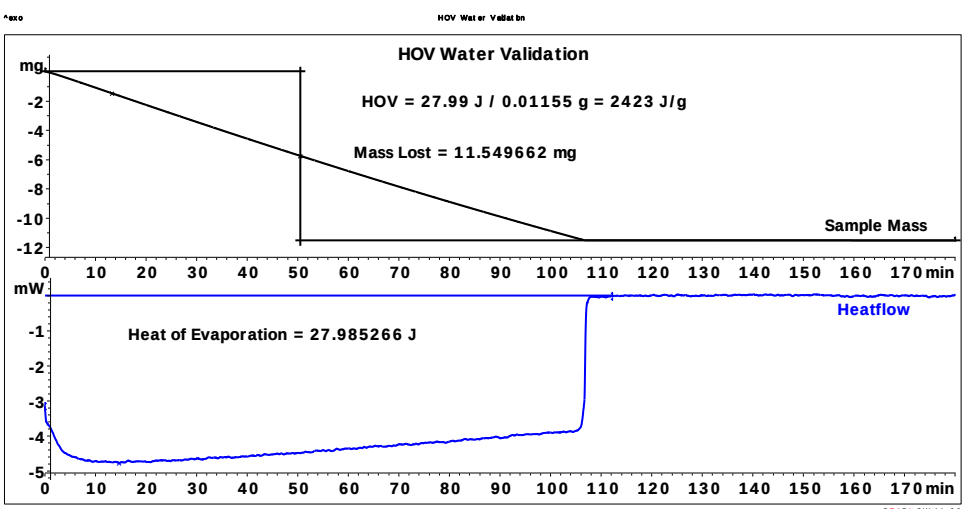

Figure 11: Validation of heatflow calibration using the HOV of water.

4.11 HOV Validation with Ethanol

Ethanol was used to validate the heat flow calibration. Ethanol was selected because it has a high HOV (918 J/g) and it was blended to make Gasoline-Ethanol blends for FACE Gasoline A and H. The TGA/DSC plots are shown in Figure 12. The heat flow integral was 7.036737793 J

and the mass loss was 0.007546074 g giving a HOV of 932.503 J/g. The literature value is 918 J/g (NIST). The result is 1.6 % higher than the NIST value, which was deemed acceptable.

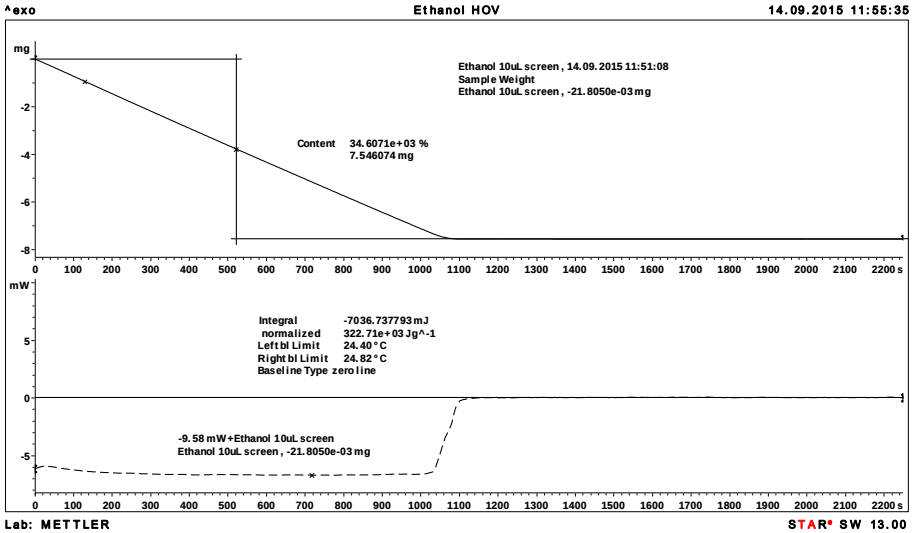

Figure 12: Validation using the HOV of Ethanol.

4.12 HOV Validation with Isooctane

A second standard liquid was selected to validate the heatflow calibration with a material that has a low HOV. In this way, one is certain that the calibration is validated over the range of HOVs to be tested in this work. The liquid selected was isooctane, which has a low HOV (307 J/g) and is one of the major compounds found in gasoline. The TGA/DSC plots are show in Figure 13. The heat flow integral was 10.038 J and the mass loss was 0.03069 g giving a HOV of 327.1 J/g. The literature value is 307 J/g (NIST). The result is 6.5 % higher than the NIST value, which was deemed acceptable.

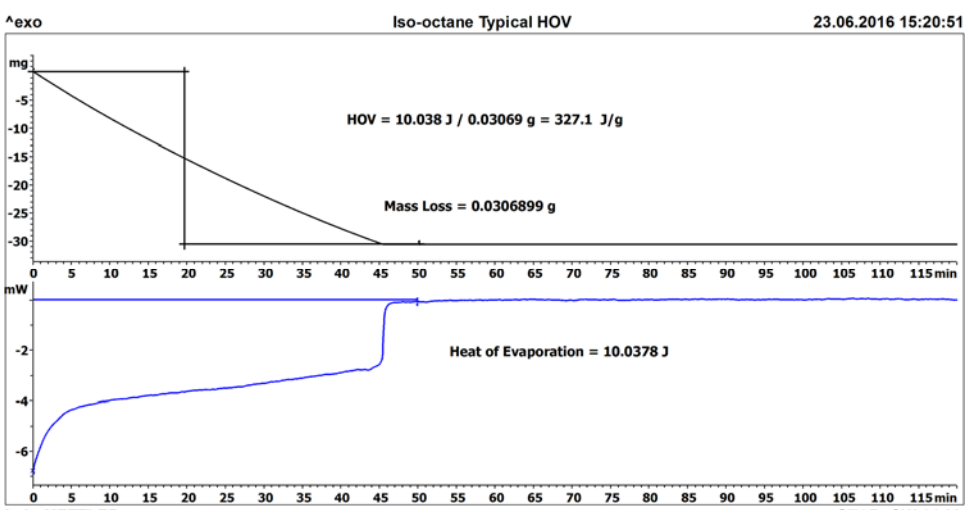

Figure 13: Validation using the HOV of isooctane.

4.13 Gasoline/Ethanol Mixture Preparation

The empty ampoule and lid were weighed. The gasoline used for the mixture (FACE A or H) was added to the ampoule and the lid was crimped closed. The gasoline mass was determined by difference. The density of the gasoline was used to calculate the volume of the gasoline in the ampoule. The target v/v % of ethanol was used to calculate the volume of ethanol needed. The syringe was used to inject the needed volume of ethanol into the ampoule. The filled ampoule was weighed again. The mass of ethanol was determined by difference. All of the mixtures prepared in this work were prepared by v/v %, but the w/w % was also calculated, data are summarized in Table 4. The testing conditions for these samples, as well as those for other liquids are summarized in Table 5.

Table 4: Gasoline-Ethanol Mixture Compositions

Material	Target Ethanol	Composition	Composition
	(v/v %)	(v/v %)	(w/w %)
FACE A & 10% Ethanol	10	11.1	11.5
FACE A & 15% Ethanol	15	14.8	14.2
FACE A & 30% Ethanol	30	29.5	33.0
FACE H & 10% Ethanol	10	9.91	10.4
Face H & 15% Ethanol	15	15.1	15.6
FACE H & 30% Ethanol	30	30.0	32.6

Table 5: Testing Conditions

Material	Crucible	Volume	N2 Flow Rate	Isothermal Time
	(µL)	(µL)	(mL/min)	(mins)
Water	40	10	50	120
Ethanol	100	30	25	90
Toluene	100	20	100	90
Iso-Octane	100	50	20	120
n-Octane	40	20	25	80
FACE Gasoline A	100	50	15	80
FACE A & 10% Ethanol	100	15.8 mg	25	90
FACE A & 15% Ethanol	100	16.4 mg	25	90
FACE A & 30% Ethanol	100	15.4 mg	25	90
FACE Gasoline D	40	20	100	180
FACE Gasoline H	40	10	200	180
FACE H & 10% Ethanol	40	7.3 mg	200	180
Face H & 15% Ethanol	40	6.4 mg	200	180
FACE H & 30% Ethanol	40	10	200	180

5. Results

The measured HOV values from all test runs of all liquids tested are included in Tables 6 - 17, with a summary of average values in Table 18.

5.1 HOV of Toluene

Table 6: HOV of Toluene

Run #	Enthalpy	Mass Loss	HOV
	(J)	(g)	(J/g)
1	9.3301	0.022724	410.58
2	5.5356	0.013507	409.85
3	6.1786	0.014504	426.00
4	5.4096	0.012460	434.15
5	7.1129	0.016865	421.76
Average			420.47
Std Devi			10.37

5.2 HOV of Isooctane

Table 7: HOV of Isooctane

Run #	Enthalpy	Mass Loss	HOV
	(J)	(g)	(J/g)
1	9.2750	0.028849	321.50
2	8.8297	0.027308	323.34
3	8.7399	0.026904	324.86
4	8.5381	0.026460	322.68
5	8.7216	0.027145	321.30
Average			322.74
Std Devi			1.46

5.3 HOV of n-Octane

Table 8: HOV of n-Octane

Run #	Enthalpy	Mass Loss	HOV
	(J)	(g)	(J/g)
1	3.5675	0.0098741	361.30
2	3.5678	0.00987408	361.33
3	3.1070	0.0087123	356.63
4	4.1589	0.011582	359.10
5	4.3699	0.011799	370.37
Average			361.75
Std Devi			5.19

5.4 HOV of FACE Gasoline A

Table 9: HOV of FACE Gasoline A

Run #	Enthalpy	Mass Loss	HOV
	(J)	(g)	(J/g)
1	4.6239	0.013331	346.85
2	3.4947	0.010369	337.03
3	7.1117	0.021006	338.55
4	6.9816	0.019874	351.30
5	7.3696	0.020716	355.74
Average			345.89
Std Devi			8.06

5.5 HOV of FACE Gasoline D

Table 10: HOV of FACE Gasoline D

Run #	Enthalpy	Mass Loss	HOV
	(J)	(g)	(J/g)
1	3.8739	0.010577	366.26
2	3.8795	0.010606	365.77
3	4.0934	0.011392	359.31
4	4.4904	0.012207	367.85
5	3.8788	0.010731	361.44
Average			364.13
Std Devi			3.59

5.6 HOV of FACE Gasoline H

Table 11: HOV of FACE Gasoline H

Run #	Enthalpy	Mass Loss	HOV
	(J)	(g)	(J/g)
1	2.3334	0.0060268	387.18
2	2.3966	0.0059570	402.31
3	2.5244	0.0066250	381.05
4	2.5173	0.0062428	403.24
5	2.1856	0.0064003	341.48
Average			383.05
Std Devi			25.14

5.7 HOV of FACE Gasoline A with 10%Ethanol

The gasoline-ethanol mixture was prepared as described previously and the resulting mixture contained 11.5 w/w% and 11.1 v/v% ethanol.

Table 12: HOV of FACE Gasoline A with 10% Ethanol

Run #	Enthalpy	Mass Loss	HOV
	(J)	(g)	(J/g)
1	6.2531	0.015461	404.44
2	6.3205	0.015800	400.03
Average			402.24

5.8 HOV of FACE Gasoline A with 15% Ethanol

The gasoline-ethanol mixture was prepared as described previously and the resulting mixture contained 14.2 w/w% and 14.8 v/v% ethanol.

Table 13: HOV of FACE Gasoline A with 15% Ethanol

Run #	Enthalpy	Mass Loss	HOV
	(J)	(g)	(J/g)
1	7.0808	0.015998	442.61
2	7.1502	0.016438	434.98
Average			438.79

5.9 HOV of FACE Gasoline A with 30% Ethanol

The gasoline-ethanol mixture was prepared as described previously and the resulting mixture contained 33.0 w/w% and 29.5 v/v% ethanol.

Table 14: HOV of FACE Gasoline A with 30% Ethanol

Run #	Enthalpy	Mass Loss	HOV
	(J)	(g)	(J/g)
1	9.1638	0.016799	545.50
2	8.2521	0.015426	534.95
Average			540.23

5.10 HOV of FACE Gasoline H with 10% Ethanol

The gasoline-ethanol mixture was prepared as described previously and the resulting mixture contained 10.4 w/w% and 9.9 v/v% ethanol.

Table 15: HOV of FACE Gasoline H with 10% Ethanol

Run #	Enthalpy	Mass Loss	HOV
	(J)	(g)	(J/g)
1	2.0108	0.0051282	392.11
2	3.1224	0.0073733	423.47
Average			407.79

5.11 HOV of FACE Gasoline H with 15% Ethanol

The gasoline-ethanol mixture was prepared as described previously and the resulting mixture contained 15.6 w/w% and 15.1 v/v% ethanol.

Table 16: HOV of FACE Gasoline H with 15% Ethanol

Run #	Enthalpy	Mass Loss	HOV
	(J)	(g)	(J/g)
1	2.2106	0.0053148	415.93
2	2.8931	0.0063932	452.53
Average			434.23

5.12 HOV of FACE Gasoline H + 30% Ethanol

The gasoline-ethanol mixture was prepared as described previously and the resulting mixture contained 32.58 w/w% and 30.00 v/v% ethanol.

Table 17: HOV of FACE Gasoline H with 30% Ethanol

Run #	Enthalpy	Mass Loss	HOV
	(J)	(g)	(J/g)
1	3.23571	0.0053515	604.64
2	2.4977	0.0046541	536.67
3	3.4409	0.0056419	609.88
4	3.4057	0.0055570	612.85
5	3.7873	0.0057993	653.06
Average			603.42
Std Devi			41.988

5.13 Summary of Average HOV Results

Table 18: Summary of HOV Results

Material	Average HOV	Standard Deviation	Literature Average HOV	Literature Standard Deviation
	(J/g)	1 σ	(J/g)	1 σ
Water		b	2442	4
Ethanol		c	918	9
Toluene	420	10	402	32
Isooctane	323	1	307	2
n-Octane	362	5	359	35
FACE Gasoline A	346	8	na	na
FACE A & 10% Ethanol	402	a	na	na
FACE A & 15% Ethanol	439	a	na	na
FACE A & 30% Ethanol	540	a	na	na
FACE Gasoline D	364	4	na	na
FACE Gasoline H	383	25	na	na
FACE H & 10% Ethanol	408	a	na	na
FACE H & 15% Ethanol	434	a	na	na
FACE H & 30% Ethanol	603	42	na	na

Notes: 'na' is not available, 'a' is not available because only two runs were made, 'b' sample was used as the calibrant, 'c' sample was used as the validation of calibration.

The HOV results for the samples are summarized in Table 18. Figures 14 and 15 show the test results of the blends of ethanol with FACE gasolines A and H, respectively, in graphic form. The blue diamonds are the actual data. The black line, in each Figure, is the theoretical straight line if the HOV of the mixtures are the linear sums of the fractions of FACE Gasoline HOV and pure ethanol HOV. As one can also see from these graphs, ethanol has a significant impact on the HOV of the mixture. These HOV values should be considered in the future design of internal combustion engines in order to maximize fuel efficiency. For the blends of FACE Gasolines A and H with ethanol, the linear sums of the fractional HOV for each component is a good estimate of HOV of a mixture.

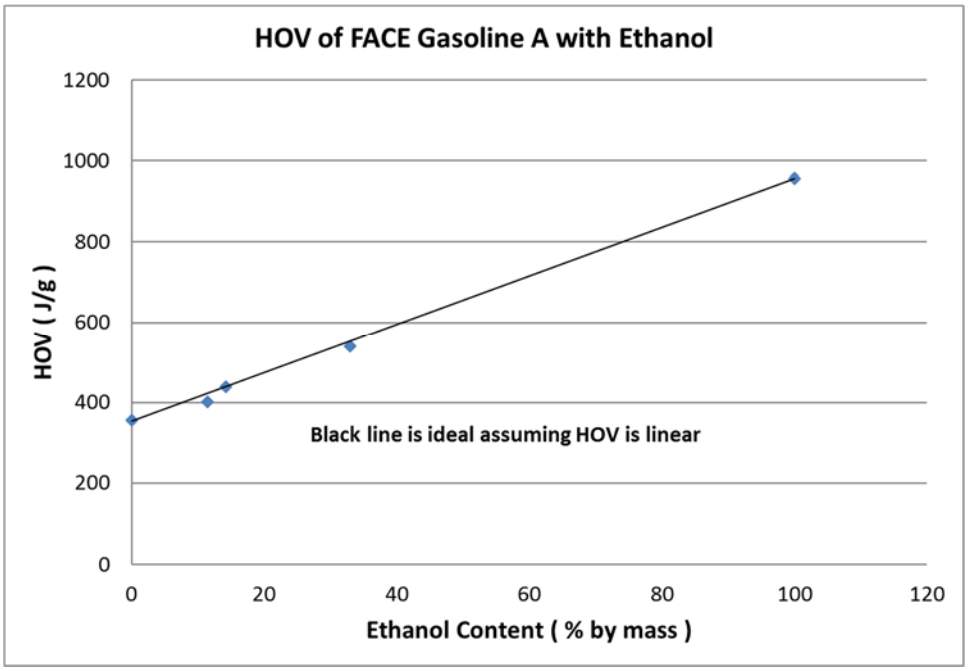

Figure 14: HOV versus ethanol content in FACE Gasoline A. The black line is the theoretical straight line if the HOV of the mixtures are the linear sums of the fractions of FACE Gasoline A and ethanol.

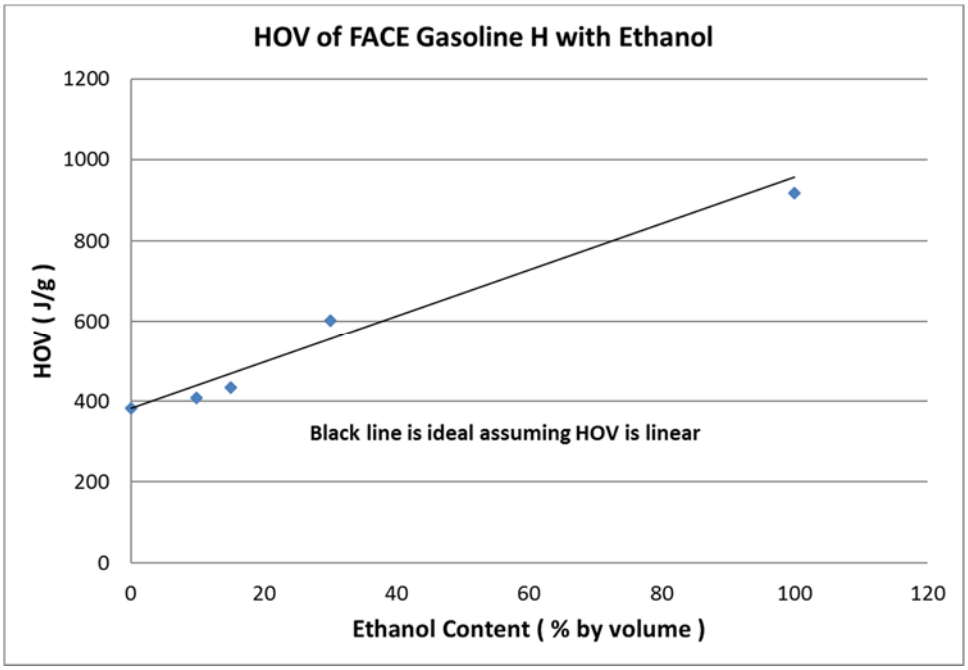

Figure 15: HOV versus ethanol content in FACE Gasoline H. The black line is the theoretical straight line if the HOV of the mixtures are the linear sums of the fractions of FACE Gasoline H and ethanol.

6. Conclusions

The HOV measurements of pure compounds, three of the FACE gasolines, and two of the FACE gasolines blended with ethanol were easily performed on a standard combination TGA-DSC instrument, without modifications. The time to heat/cool the instrument was eliminated by using the recirculating constant temperature water bath to hold the furnace at 25 °C through all of the testing. Careful heatflow calibration using HOV standards, such as water, was required in order to obtain most accurate results.

There is an inherent variance to this HOV measurement, as with all measurements. There did not seem to a correlation between high variance and any sample nor test method conditions. The only observation from this work is that the sample needs to be prepared, crimped in the crucible and placed in the TGA as quickly as possible. This seems to be especially true for distillate derived samples such as gasoline. Multiple runs (3 to 5) are recommended in order to get the best average HOV value.

The traditional HOV test, which uses the Clausius-Clapeyron equation [1, 2], can only rigorously be used for pure compounds, not multi-component distillates such as gasoline. This approach (e.g., used in ASTM E2071 [3]) gives the HOV for the compound in J/mol at its normal boiling point. Internal combustion engine engineers prefer the HOV in the units of energy per mass, such as J/g, and at a temperature other than the boiling point, such as 25 °C in this work. The TGA-DSC test for HOV gives the results at an exact temperature (25 °C in this case) as required by the application. The test also gives results in the preferred units of J/g. The HOV of a distillate, such as gasoline, can be determined with the TGA-DSC technique used in this work.

7. References

1. Clausius, R. (1850). "Ueber die bewegende Kraft der Wärme und die Gesetze, welche sich daraus für die Wärmelehre selbst ableiten lassen" [On the motive power of heat and the laws which can be deduced therefrom regarding the theory of heat]. *Annalen der Physik* (in German) **155**: 500–524 (1850).
2. Clapeyron, M. C. (1834). "Mémoire sur la puissance motrice de la chaleur". *Journal de l'École polytechnique* (in French) **23**: 153–190 (1834).
3. ASTM E2071, *Standard Practice for Calculating Heat of Vaporization or Sublimation from Vapor Pressure Data,* 2000.
4. K.S. Alexander, D. Dollimore, and T.V. Sorokina, Thermochimica Acta, 2002, 392-393, 315-321.
5. M. Houska, et. al., J. Food Engineering, 2008, 87, 59-63.
6. Bauer, W-D., 'Heat transfer and mixture vaporization in intake systems of spark ignition engines', PhD Thesis, MIT (1997).
7. API Publication No. 4261, 'Alcohols and Ethers: a Technical Assessment of Their Application as Motor Fuels and Fuel Components', 3rd Edition, June 2001.
8. Balabin, R.M., Syunyaev, R.Z., and Karpov, S.A., 'Molar enthalpy of vaporization of ethanol-gasoline mixtures and their colloidal state', FUEL, 86, 323-327 (2007).
9. Kar, K., Last, T., Haywood, C., and Raine, R., 'Measurement of vapor pressure and enthalpies of vaporization of gasoline and ethanol blends and their effects on mixture preparation in an SI engine', SAE Int. J. Fuels Lubr., 1(1), SAE 2008-01-0317, 132-144 (2008).
10. Cannella, W., Foster, M., Gunter, G., and Leppard, W., "FACE Gasolines and Blends with Ethanol: Detailed Characterization of Physical and Chemical Properties", CRC Report No. AVFL-24, July 2014.

Appendices

Appendix A: Experimental Variables that Affect the HOV Measurement

Type of Orifice

Pinhole versus Screen

Water was run with a pinhole lid and the screen to detect the difference. The evaporation rate was lower with the pinhole, as expected. This lower evaporation rate made the heatflow signal smaller. This reduced the signal to baseline noise which increase the HOV variance. The HOV for water with the screen was 2162 J/g and with the pinhole was 1983 J/g. The absolute values are not meaningful since they were performed before proper heat flow calibration was completed. The differences are important. The screen is better at capturing more of the heat and gives a larger heatflow value, and a larger HOV. The pinhole will bias the results toward the lower vapor pressure components of the gasoline sample and the screen will bias toward the higher vapor pressure components. Figure A1 shows the mass loss of FACE gasoline H with different size orifices. The FACE H sample did not completely evaporate at 25 °C even after 3 hours. In a case such as this, one would use a smaller volume of the gasoline sample. All samples run for this report had a complete evaporation by the end of the test.

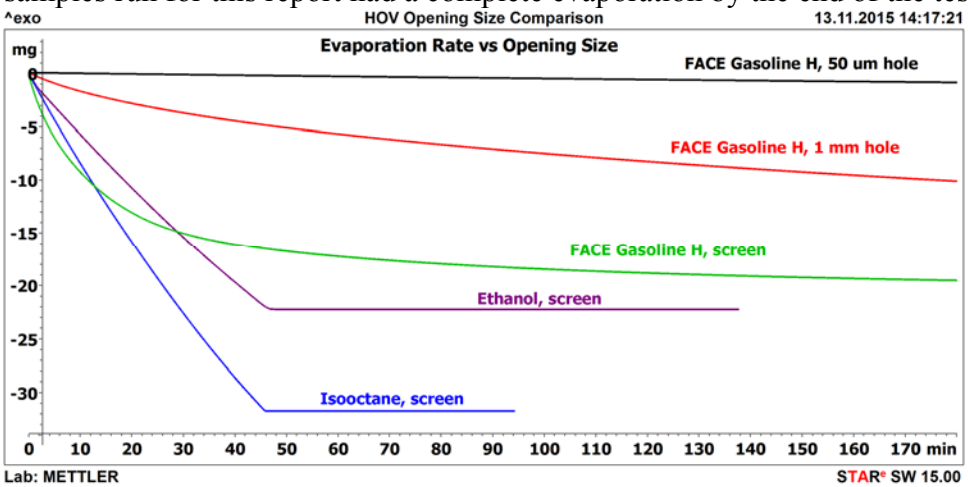

Figure A1: Evaporation rate versus opening size. FACE gasoline H is the slowest of the gasolines to evaporate. It requires a large opening to evaporate promptly. Pure materials, such as ethanol and isooctane, evaporate to a flat baseline in the mass curve.

Variables that do not affect HOV

"Crucible"

Both crucibles have the same internal diameter. They only vary in height. These variables do not correlate with the measurement offset from literature. The smaller volume 40 µL crucible will increase the rate of evaporation. This will make the heat flow signal larger. This makes the experiment for low vapor pressure materials faster, but the crucible alone will not improve the variance. An extensive analysis of effect of crucible choice on the HOV results was beyond the scope of this project. The selection of crucible volume and sample volume was a simple 'trial and error' approach.

"Gas Flow Rate"

The heat flow baseline is not affected by this flow rate. Just like the crucible, the gas flow rate will increase the rate of evaporation, but it alone will not improve the variance.

"Volume Used"
As long as there is sufficient material in the crucible to give a large enough heatflow signal (at least 4 mW more endothermic than the baseline), then the "volume used" does not affect the HOV.

Variables that affect HOV
"Mass Loss"
This is an important measurement because it is ½ of the HOV equation. As long as the mass of sample put in the crucible is large enough, 10 to 20 mg, the variance of this measurement will be low.

"Enthalpy"
There are two parts to the enthalpy calculation, the area and the value of zero het flow. I have been using a best line fit, of zero order, to the last 30 to 60 minutes of the experiment. I subtract that value from the original data. Then I integrate the heat flow to the zero heat flow value. I calculate the mass loss and enthalpy over the same time window. Error is introduced when the sample does not completely evaporate during the test. In this case the enthalpy is too low which causes the HOV to be too low.

"Time"
The time to reach a baseline is dependent on the vapor pressure, crucible type and purge rate. I have gotten a low variance for all samples that had a time from 50 to 70 minutes, with the exception of Toluene.

"Heat Flow"
The larger heat flow gives lower variance. Since enthalpy is calculated from the heat flow curve, a large heat flow gives a large enthalpy and this gives a lower variance HOV, with the exception of Toluene.

"Evaporation from the Sealed Vials"
I tested the long term evaporation rate of each gasoline sample from the crimped ampoules. I reweighed each ampoule over several days. The results are shown in Figure A2. The goal of this is to given me an 'expiration date' for the gas/ethanol mixtures. I will use 60 days as my 'expiration' date, but I will reweigh each ampoule prior to taking a new aliquot from the ampoule. I will make a new sample after it has lost 0.5% of its original weight.

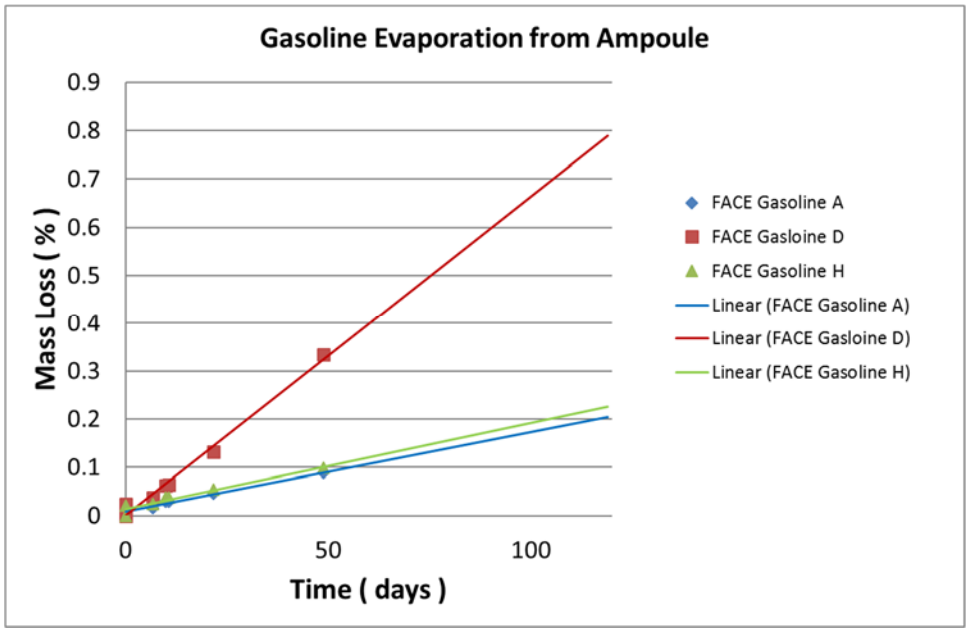

Figure A2: Room temperature mass evaporation through crimped ampoules.